Biochemical Characterization of Glutathione Transferase YliJ from *Escherichia coli*

by

Collins Aboagye

Submitted in Partial Fulfillment of the Requirements

for the Degree of

Master in Science

in the

Chemistry

Program

YOUNGSTOWN STATE UNIVERSITY

December, 2015

Biochemical Characterization of Glutathione Transferase YliJ from *Escherichia coli*

Collins Aboagye

I hereby release this thesis to the public. I understand that this thesis will be made available from the OhioLINK ETD Center and the Maag Library Circulation Desk for public access. I also authorize the University or other individuals to make copies of this thesis as needed for scholarly research.

Signature:

Collins Aboagye, Student Date

Approvals:

Dr. Nina V. Stourman, Thesis Advisor Date

Dr. Michael Serra, Committee Member Date

Dr. Josef Simeonsson, Committee Member Date

Dr. Salvatore A. Sanders, Dean of Graduate Studies Date

Abstract

Glutathione transferases, or GSTs, protect cellular components from the dangers posed by electrophiles by catalyzing the conjugation of the electrophilic molecules with glutathione. This makes GSTs very successful detoxifying agents in most organisms. Glutathione transferase YliJ, also known as GstB, has been postulated to catalyze the glutathione mediated dehalogenation of bromoacetate. The objective of this research is to develop a simple purification procedure for YliJ, design a safe method for assaying YliJ activity, characterize YliJ, and to search for other potential substrates for YliJ. YliJ was overexpressed in *E. coli* cells and purified using ammonium sulfate precipitation and ion-exchange chromatography. The presence and purity of YliJ was verified by sodium dodecyl sulfate-polyacrylamide gel electrophoresis. YliJ has a K_M of 1.60 mM, a k_{cat} of 175.0 s^{-1} and a catalytic efficiency of 1.09×10^5 $M^{-1}s^{-1}$ for GSH when conjugated to bromoacetate. In comparison, YliJ has a K_M of 0.1753 mM, a k_{cat} of 155.3 s^{-1}, and a catalytic efficiency of 8.86×10^4 $M^{-1}s^{-1}$ for GSH when conjugated to iodoacetate. *E. coli* cells expressing YliJ protein and the knockout strain BW25113Δ*yliJ* lacking YliJ were tested for sensitivity to halogenated compounds and antibiotics. The results strongly support the suggestion that a small molecule containing a carboxylate moiety could be the physiological substrate of YliJ.

Acknowledgements

I would first like to thank Dr. Nina Stourman for being my advisor. I am very grateful that she accepted me in her lab. She has directed my research with the upmost interest and patience making my experience very enjoyable. She has instilled in me the knowledge and shown me the needed techniques necessary to carry out my research. Her hard work, dedication and professional encouragement inspired me to develop and learn the work ethic needed to complete this work. I can't thank her enough for everything she has done for me. I would also like to express my gratitude to my committee members Dr. Michael Serra and Dr. Josef Simeonsson for their advice and for accepting to be on my committee.

I would like to thank my family and friends both home and abroad for their tremendous support, love, and understanding during my most stressful times. I would like to acknowledge the members of my laboratory, those who have long moved on to other endeavors and those who have yet to complete their studies. I also acknowledge Linda Sui for the immense role she has played in my research.

Finally, I would like to acknowledge the Youngstown State University Chemistry Department for providing me the opportunity to learn, and also providing a place, equipment, and chemicals needed to complete my research.

Table of Contents

List of Figures

List of Tables

List of Abbreviations

E. coli	*Escherichia coli*
GSH	glutathione
GST	glutathione transferase
DNA	deoxyribonucleic acid
EDTA	ethylenediaminetetraacetic acid
IPTG	isopropyl-beta-D-thiogalactopyranoside
TEMED	tetramethylethylenediamine
MES	2-(N-morpholino)ethanesulfonic acid
kDa	kilodalton
$O.D_{600}$	optical density at 600 nm
nm	nanometers
cm	centimeters
µL	microliters
mL	mililiters
mM	milimolar
µM	micromolar
SDS-PAGE	sodium dodecyl sulfate-polyacrylamide gel electrophoresis
SOC	super optimal broth with catabolite repression
SOB	super optimal broth
LB	Luria- Bertani medium
pI	isoelectric point

Chapter 1: Introduction

Structure, Properties, and Role of Glutathione

Glutathione (GSH) is a tripeptide known as γ-L-glutamyl-L-cysteinylglycine (Figure 1.1) with a peptide linkage between the γ-carboxyl group of the glutamate side-chain and the amino group of cysteine. The presence of the γ-glutamyl bond protects the tripeptide from degradation by intracellular peptidases, while the sulfhydryl group of cysteine can serve as an electron donor, endowing glutathione with reducing properties and the ability to remove free radicals[1].

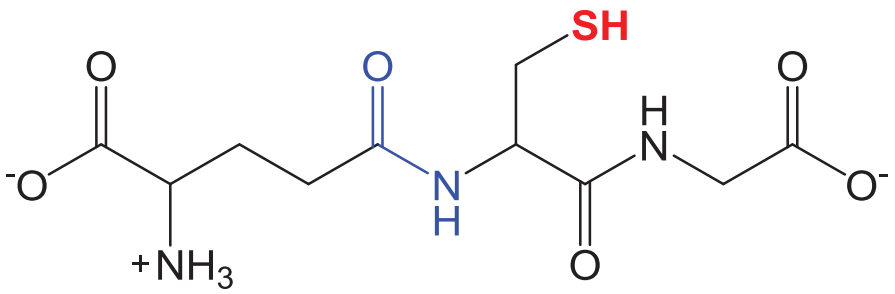

Figure 1.1*: Structure of the tripeptide glutathione*

Glutathione is the most abundant low molecular mass thiol compound found in nearly all cellular organisms where it plays major roles in the defense against oxidative damage and in signaling pathways[2]. GSH also has an important role in the detoxication of xenobiotics, cell homeostasis, and radioprotection. Usually, glutathione acts as a nucleophile that reacts with electrophilic centers of a variety of compounds. GSH can be used to maintain a thiol/disulfide redox potential by acting as a buffer[2]. Also acting as

reducing agent, glutathione can reduce hydrogen peroxide through a redox reaction where oxygen acts as an electron acceptor[3]. In this reaction, two molecules of GSH are oxidized, forming a disulfide bond. The enzyme glutathione reductase usually reduces the oxidized glutathione disulfide, GSSG, molecules back to reduced GSH[3].

Relatively high concentrations of GSH are found in all eukaryotic cells unlike in prokaryotic cells where GSH is found mostly in Gram-negative bacteria including *Escherichia coli.* GSH is absent in most Gram-positive bacteria except some *Streptococcus* and *Enterococcus* species[4, 5]. Some Gram-positive bacteria, however, are able to synthesize GSH or consume GSH from the growth medium. Bacteria such as *Haemophilus influenzae* and *Lactococcus lactis* cannot synthesize glutathione, but they can take GSH up from the medium. This helps increase their resistance to hydrogen peroxide[6, 7]. Other low molecular weight thiols which perform similar functions as GSH are synthesized by non-GSH producing facultative aerobic and anaerobic prokaryotes[5, 8,].

In eukaryotic cells glutathione plays a key role in defense against oxidative stress by acting as a cofactor of both selenium dependent and independent glutathione peroxidases[9]. Often, selenium is needed in order for glutathione to reduce free radicals while NADPH and riboflavin are needed to reduce oxidized glutathione back to its reduced form. One of the general features of oxidative stress in eukaryotes is the drop in the GSH/GSSG ratio due to high rates of GSH oxidation. The role of glutathione in response to oxidative stress greatly varies in eukaryotes and bacteria. This is because some bacteria including *E. coli* do not possess the enzyme glutathione peroxidase which is mainly responsible for protecting organisms from oxidative damage[8].

The metabolism of GSH in human cells differs from that of bacteria and this makes it a good potential target for antibacterial agents[3]. Glutathione is one of the metabolites in *E. coli*. The ability of *E. coli* to grow in anaerobic conditions is aided by the role of glutathione in regulating the potassium release channels of the bacteria. Glutathione also plays a key role in detoxifying superoxide oxidant within the bacteria via redox reactions[10]. Glutathione can be conjugated to various electrophilic compounds including a non-natural toxicant, bromoacetate, in a dehalogenation process to form glutathione-S-acetate, a reaction catalyzed by glutathione transferase YliJ[11].

Glutathione Transferases (GSTs) Superfamily

Glutathione transferases (GSTs) produced mostly by aerobic organisms belong to a multifunctional family of proteins. They play a major role in protecting cells against a wide variety of exogenous and endogenous small molecule toxicants[12]. This family is also known as the Phase II detoxication enzymes that catalyze the conjugation of glutathione to a great variety of electrophilic compounds making the target molecules more water-soluble and thus facilitating their excretion from the cell. This renders GSTs very successful detoxifying agents in most organisms. GSTs are extensively distributed in nature and are present in both eukaryotes and prokaryotes. GSTs can be categorized into at least four major families of proteins, namely cytosolic GSTs, microsomal GSTs, mitochondrial GSTs, and bacterial fosfomycin-resistance enzymes[13, 14]. With respect to quaternary structure, the cytosolic GSTs are hetero- or homodimeric water soluble proteins while the microsomal GSTs are trimeric and membrane bound proteins[15].

Average size of an individual cytosolic GST subunit has been found to be about 25 kDa. Based on the chemical, physical, and structural properties, the cytosolic GSTs (cGSTs) have been further divided into numerous divergent classes[1, 3, 16]. The second GST sub-family constitutes membrane-bound transferases called membrane-associated proteins involved in ecosanoid and glutathione metabolism (MAPEG). However, these have no similarity to the soluble mitochondrial GSTs also called kappa GSTs which have been characterized in eukaryotes[17, 18]. Representatives of all three sub-families are also found in prokaryotes. The fourth family is found only in bacteria.

Substrates of Glutathione Transferase Isoenzymes

The major function of the various GST enzymes in cellular organisms has been identified to serve as a line of defense against numerous harmful chemicals produced endogenously and in the environment. Generally, GST enzymes catalyze the conjugation of reduced glutathione to a wide variety of electrophilic chemical compounds. Compounds that are often conjugated to GSH by the action of GST include halogenated aromatic and aliphatic compounds, isothiocyanates, α,β-unsaturated carbonyls, quinones, and polycyclic aromatic hydrocarbon epoxides derived from the catalytic actions of Phase I cytochrome P-450s as well as numerous by-products of oxidative stress (Figure 1-2)[19, 20]. Some of the other GST substrates are compounds which contain electrophilic centers such as organic nitrate esters, chemotherapeutic agents such as chlorambucil, cyclophosphamide, melphalan, thiotepa, and the antibiotic fosfomycin[19,20] (Figure 1-3). GSTs have been identified to show remarkably broad substrate specificity

and are unusual in exhibiting several catalytic activities. GSTs possess the ability to differentiate nonsubstrate drugs and hormones.

1-Chloro-2, 4-dinitrobenzene (CDNB) is the most widely used substrate to study glutathione transferases. When conjugated to GSH, CDNB produces S-(2, 4-di-nitrophenyl)-glutathione (Figure 1-4), a compound possessing an absorbance spectrum different from that of CDNB to allow a simple spectrophotometric assay at 340 nm[21].

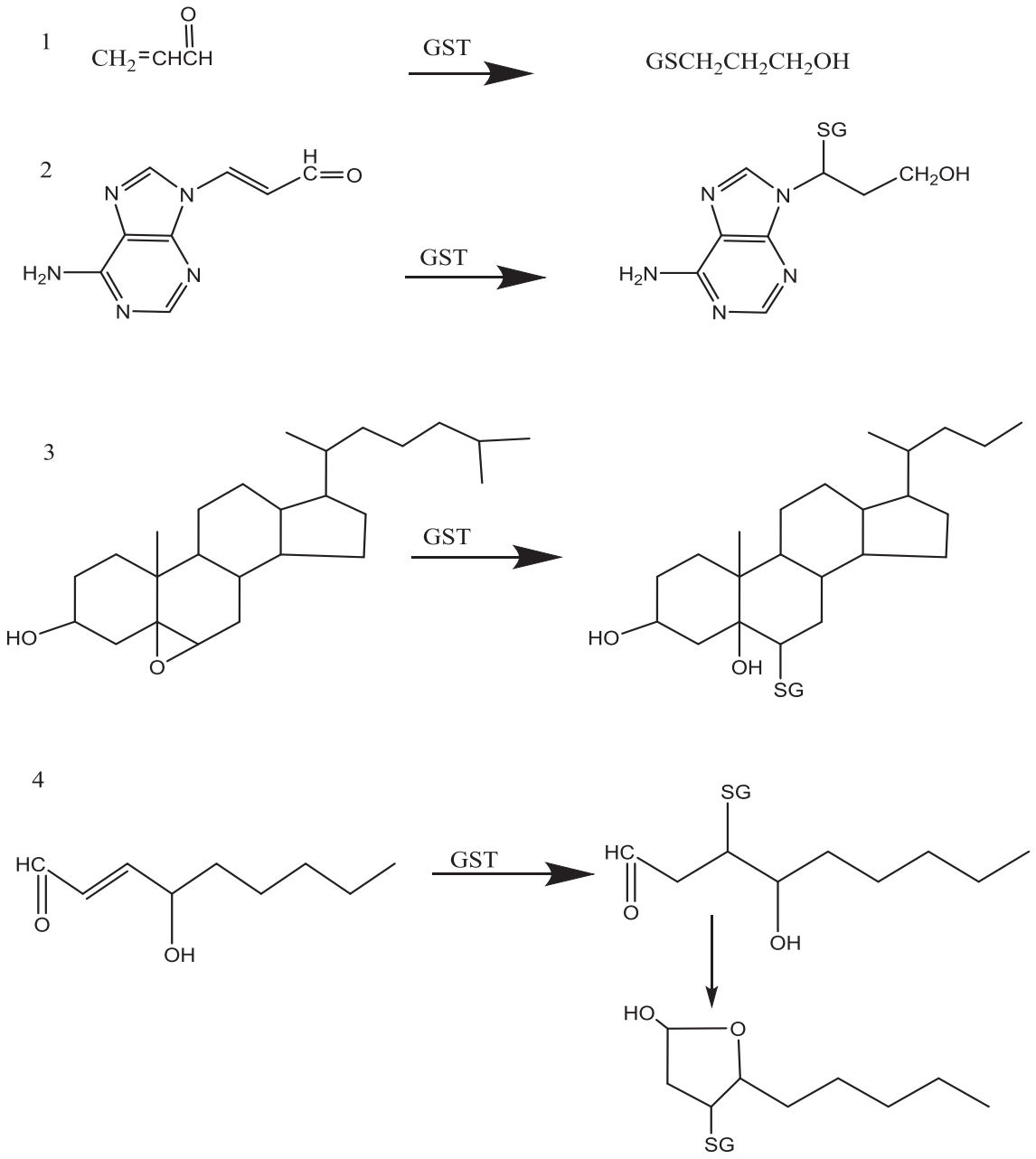

Figure 1-2. *Examples of GST substrates that are produced by oxidative stress: (1) acrolein; (2) adenine propenal; (3) cholesterol-5, 6-oxide; (4) 4-hydroxynon-2-enal. (Adapted from Hayes and Pulford (1995))*

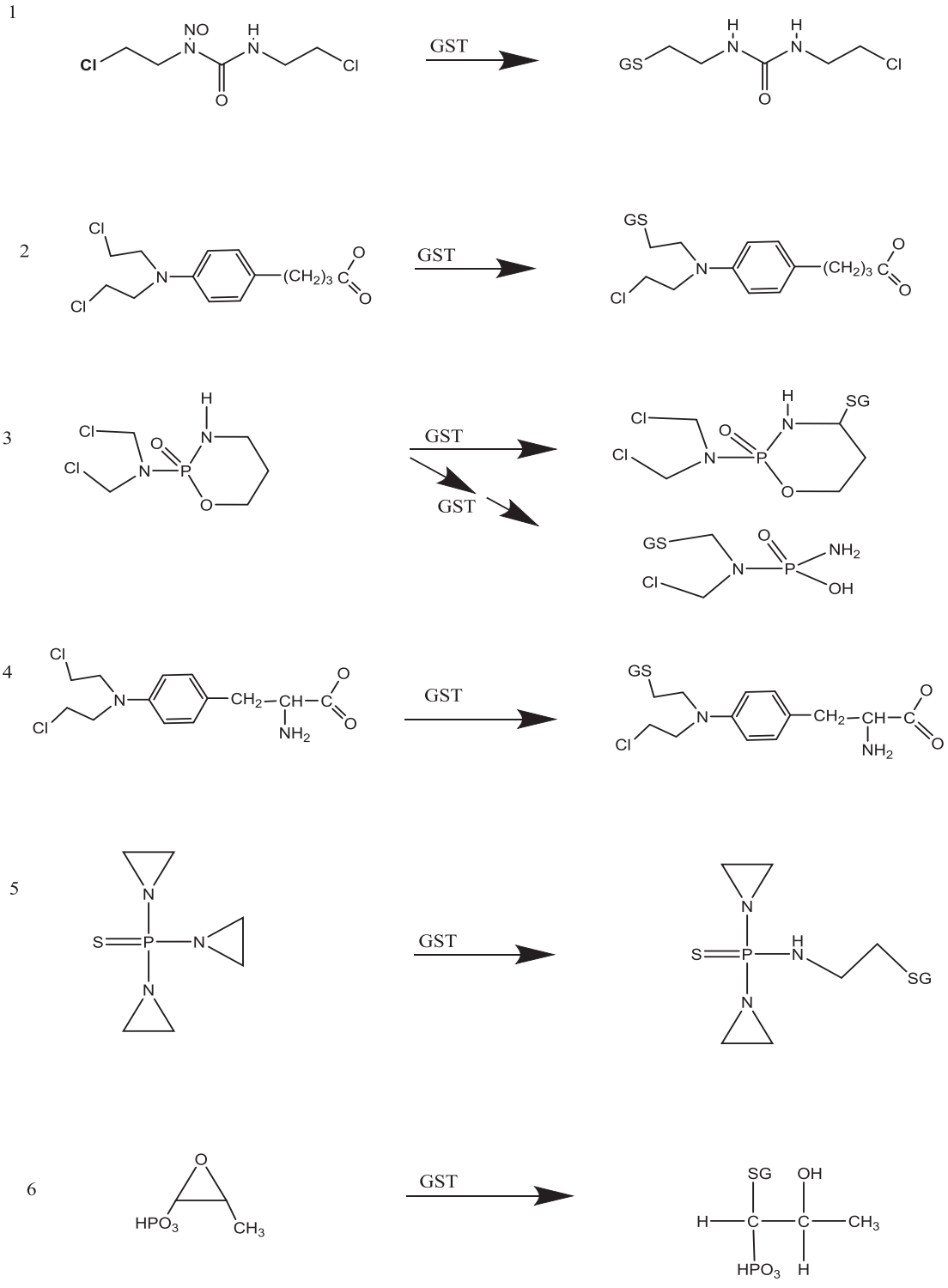

Figure 1-3. *Examples of chemotherapeutic agents that are GST substrates: (1) bis-chlorethylnitrosourea (2) chlorambucil; (3) cyclophosphamide; (4) melphalan; (5) thiotepa; (6) fosfomycin. (Adapted from Hayes and Pulford (1995))*

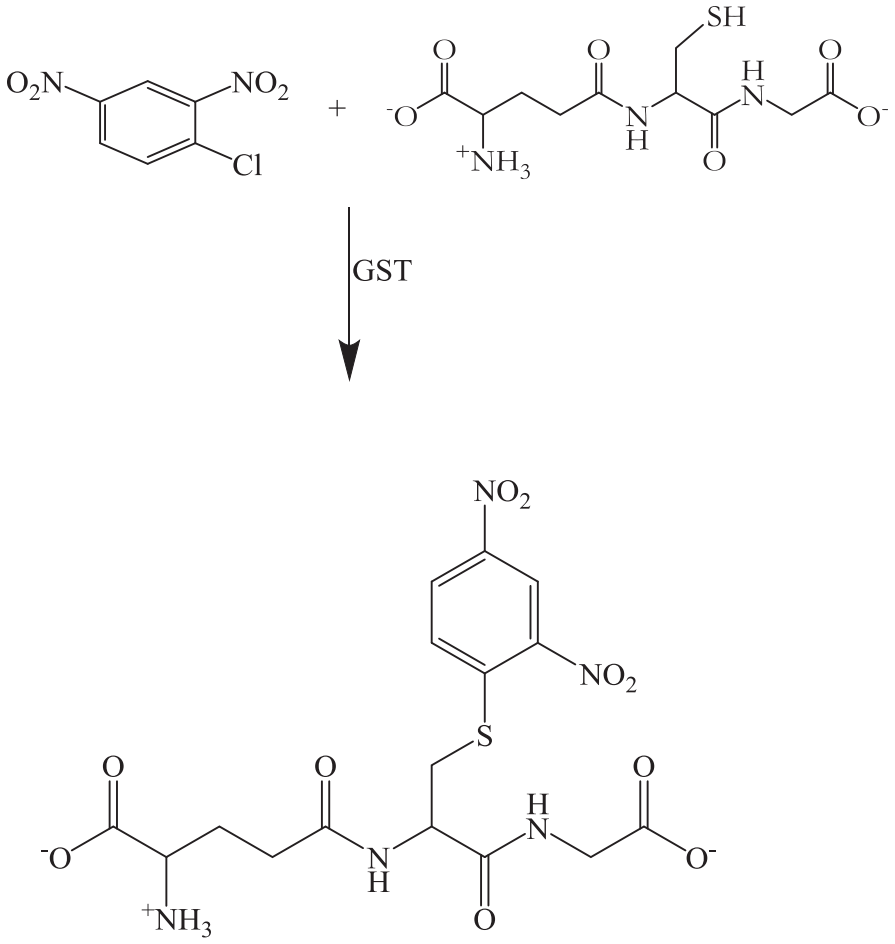

Figure 1-4. *Scheme of GST catalyzed conjugation of CDNB and GSH*

Classification of Bacterial GSTs

Glutathione transferases (GSTs) are widely distributed in nature. They are generally found in bacteria, fungi, mollusks, crustaceans, worm parasites, frogs, insects, fish, birds, plants, and mammals. The classifications used to describe GSTs in rats and humans continue to have a major impact on the study of GSTs in other organisms. This is because rats and human GSTs have been studied in the greatest detail. On the basis of the primary structures of numerous purified cytosolic GST isoenzymes from rats and

humans, five different GST classes have been identified: alpha, mu, pi, sigma, and theta. However, there are no clearly established criteria concerning the extent of sequence similarity required to place a GST in a particular class[20].

Bacterial genomes contain multiple GST-encoding genes of widely divergent sequences and unknown functions. Four different classes of cytosolic GSTs have been identified in bacteria: beta, chi, theta, and zeta. The beta class GSTs which are able to conjugate the model substrate 1-chloro-2, 4-dinitrobenzene and bind to the GSH–affinity matrix have been purified and characterized from several bacteria[22]. All beta class enzymes are characterized by the presence of a cysteine residue at the GSH binding site[22]. The first cytosolic GST of this class known as the PmGST which displayed biochemical and structural properties that distinguish it from other GSTs was isolated from *Proteus mirabilis*. Many remarkable differences in enzymatic properties are possible within the group of bacterial GSTs. For instance, K_M values for glutathione in the millimolar range are often thought to be characteristic of theta class enzymes[23].

The *E. coli* genome harbors eight predicted glutathione transferase homologues. GSH transferase homologues indicate that at least five families are represented by the eight proteins[24-26]. YfcF, YfcG, and YliJ are among the products of the identified GST homologous genes. The former (YfcF and YfcG) have been shown to exhibit GST- and GSH-dependent peroxidase activities and are involved in the defense against oxidative stress[27]. YghU, a nu class GSH transferase, has been identified to have similar structural and functional properties to those of YfcG. Thus YfcG and YghU from *E. coli* have been postulated to be the reserved members of a new class of GSH transferases that have

unique structural and functional properties. Their uncommon structural and functional properties enable them to bind and utilize GSSG or a GSH pair in a way that promotes disulfide-bond oxidoreductase reactions[28]. For instance, both enzymes (YghU and YfcG) have been shown to exhibit robust disulfide-bond reductase activity toward 2-hydroxyethyl disulfide. However, YghU has a superior activity toward organic hydroperoxides than YfcG[28]. Usually, the electrophilic side chain residues located at the N-terminal end of α-helix 1 that helps in the stabilization of the glutathione thiolate are tyrosine, serine or cysteine. The residue (tyrosine, serine or cysteine) also serves as one of the structural delineations between the various classes of GSH transferases. The first structurally confirmed examples of GSH transferase that utilizes a threonine hydroxyl group in the stabilization of the glutathione thiolates were YghU and YfcG[28].

One of the first bacterial GST to be characterized at both functional and sequence levels was dichloromethane dehalogenase from *Methylobacterium dichloromethanicum* and *Methylophilus sp*.[29, 30]. Dichloromethane dehydrogenase catalyzes the glutathione-dependent conversion of dichloromethane (DCM) to formaldehyde and two equivalents of HCl and allows certain methylotrophic bacteria to grow with DCM as the sole carbon and energy source[29].

Glutathione transferase YliJ also known as GstB, has been postulated to catalyze the glutathione mediated dehalogenation of bromoacetate as indicated in Figure 1-5 below[11]. Generally, GSTs from *E. coli* have been found to exhibit higher affinity for glutathione ($K_{M\,=}$40 µM) than GST from *Proteus mirabilis* ($K_{M\,=}$686 µM)[23].

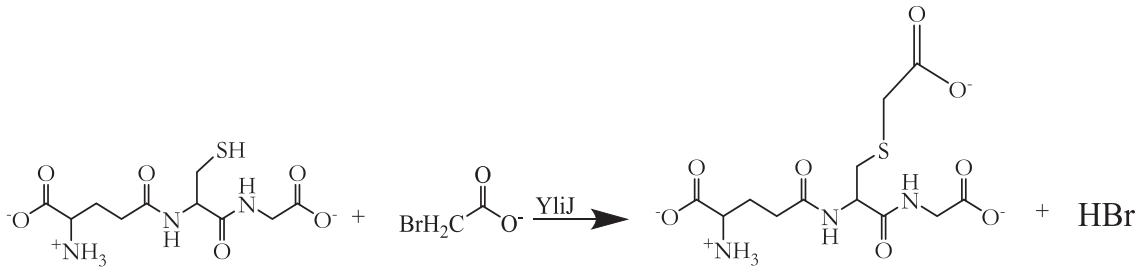

Figure1-5. *Glutathione transferase YliJ catalyzed reaction*

Properties and Functions of GSTs

Glutathione transferase enzymes play a major role in Phase II of drug metabolism. Here they contribute to cell survival by detoxication of foreign compounds. This is a bi-substrate reaction which involves reduced glutathione and the xenobiotic (foreign compound). The reduced glutathione acts as a nucleophile by attacking the electrophilic centers generated by the functional group of the foreign compounds. This reaction which is catalyzed by GST allows the xenobiotic-conjugate to be removed from the cell during Phase III of drug-metabolism, a process which requires the participation of drug transporters such as multi-drug resistance associated protein (MRP)[31]. Glutathione transferases also catalyze the reduction of peroxide-containing compounds that may otherwise be toxic to the cell[32].

Glutathione transferases play significant roles in non-enzymatic ligand binding where they are involved in a wide range of functions such as: carcinogen-detoxication (Figure 1-6) and intracellular transport of a wide spectrum of substances. Studies have shown that some members of the alpha class GST can bind covalently reactive

metabolites formed from 3-methylcholanthrene and azo-dye carcinogens[33,34]. The soluble GSTs bind to many compounds (ligands) and most often these ligands, which are normally lipophilic in nature, are not substrates for the conjugation reaction[20]. These ligands or lipophilic compounds include steroid hormones, thyroid hormones, bile acids, bilirubin, free-fatty acids, and numerous drugs[35]. Although, the biological significance of this non-covalent binding activity has been a subject of much debate, it was first proposed several years ago that the binding of steroid hormones, thyroid hormones, bile acids, and bilirubin may contribute to the transport of these compounds across the liver and enhance their elimination in the bile[20, 35].

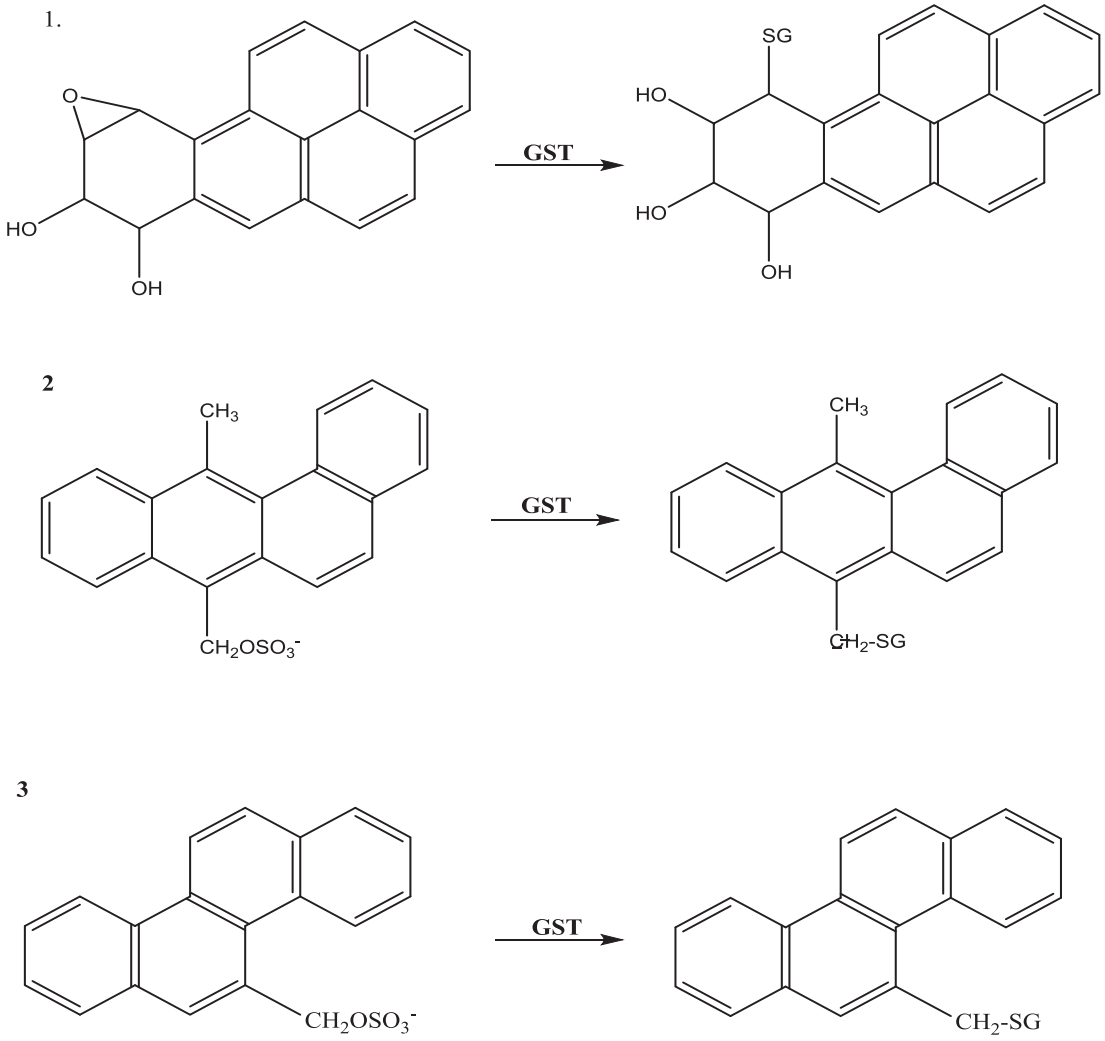

Figure 1-6. *Examples of GST catalyzed detoxification of carcinogens: (1) benzo[a]pyrene-7, 8-diol-9,1O-oxide; (2)7- hydroxymethylbenz[a]anthracenesulfate; (3) 5-hydroxymethylchrysenesulfate. (Adapted from Hayes and Pulford (1995))*

In plant cells, glutathione transferases are involved in the detoxication and transport of pesticides and herbicides. They also play important roles in the metabolism of endogenous compounds and in the protection of plant cells from pathogenic infection, often in the course of stress-related responses[36]. Usually, GSTs catalyze the

addition of reduced glutathione to electrophilic pesticides (Figure 1-8); however, they can also show hydrolytic and peroxidase activities[37].

Isomerization of many biologically important molecules involves the activities of glutathione transferases. GSTs catalyze the GSH dependent conversion of prostaglandin (PG) D_2 to either PGD_2 or PGE_2 and the isomerization of maleylacetoacetate to fumarylacetoacetate, a step in the degradation of tyrosine[38, 39]. GSTs can also catalyze *cis-trans* isomerization reactions or the movement of a double bond within a polycyclic molecule[40]. This includes the conversion of 13-*cis*-retinoic acid to all-*trans*-retinoic acid, a reaction that results in an increase in affinity of the retinoid for its receptor[41].

Despite the numerous detoxication activities of GSTs, some classes of GSTs catalyze reactions which can lead to the formation a more reactive and potentially carcinogenic intermediate (Figure 1-7)[20]. For instance, studies have shown that a member of the class theta GST family in the mouse is capable of metabolizing dichloromethane to form a highly reactive S-chloromethylglutathione conjugate[42].

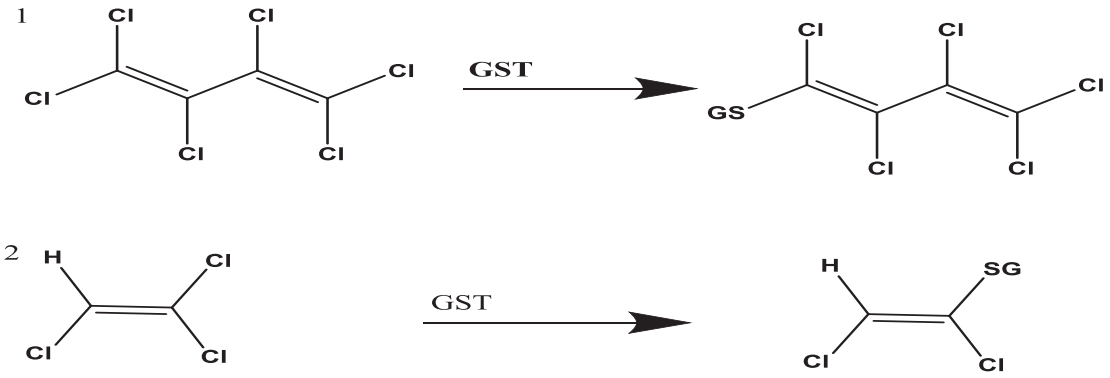

Figure 1-7. *Examples of compounds that form indirectly acting toxic GSH conjugates: (1) hexachloro-l, 3-butadiene; (2) trichloroethene. (Adapted from Hayes and Pulford (1995)*

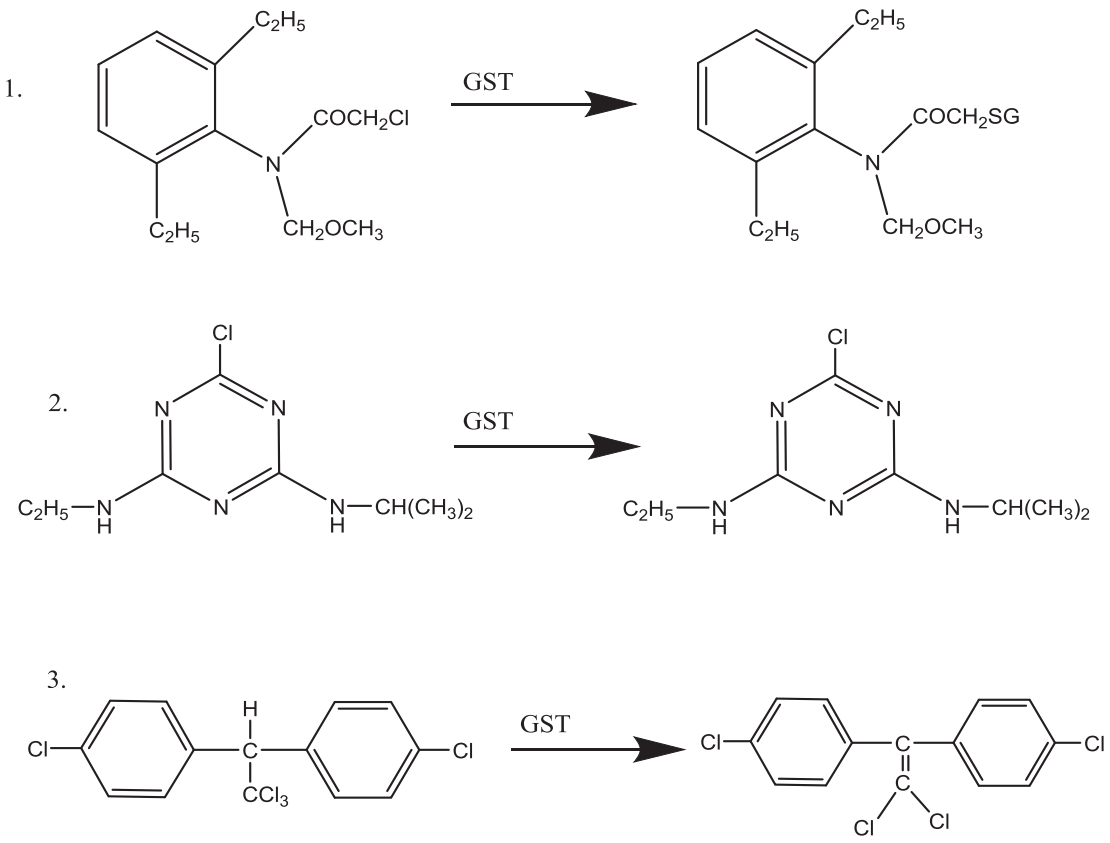

Figure 1-8. *Examples of metabolism of pesticides and environmental pollutants by GST: (1) alachlor; (2) atrazine; (3) DDT. (Adapted from Hayes and Pulford (1995))*

Potential Applications of GSTs

The compounds that can interact with members of the GST family within the same structural framework continue to be increasingly identified. As such, GST enzymes may be recruited and employed to catalyze a given conjugation reaction of interest. A large range of GST enzymes are yet to be uncovered in the bacterial world. However, some of the already characterized glutathione transferases catalyze reactions that yield products which can be used for bacterial growth. These GSTs include the bacterial DCMD, lignin β-etherase, and reductive dehalogenase enzymes[42].

Glutathione transferases can be employed in the detoxication studies of chemical compounds in bacteria. Bacterial GST enzymes can also be employed in the degradation of herbicides and further metabolism of glutathione conjugates. The general role of GST enzymes in the biological processes featuring sulfur-containing metabolites of xenobiotics makes bacterial GST enzymes an important and exciting area for research[42, 43].

Analysis of Predicted Primary Structure of YliJ

Glutathione transferase YliJ from *E. coli* is a protein that is predicted to belong to the GST superfamily. The enzyme has been shown to catalyze the glutathione-dependent dehalogenation of bromoacetate[11]. YliJ is also found to be significantly reactive with iodoacetate when compared to other halogenated compounds. This suggests that the physiological substrate of YliJ is probably a small molecule containing a carboxylate moiety[11]. The amino acid sequence of the protein was obtained from a

central repository of protein sequence *uniprot.org* and submitted to the Phyre2 web portal for protein modeling, prediction and analysis[44]. The description of the YliJ structure presented below is based on the predicted structure and similarity to other proteins.

Glutathione transferase YliJ from *E. coli* consists of 208 amino acids with a calculated isoelectric point (*pI*) of 5.05 (Figure 1-9). The molecular weight of the polypeptide from the amino acid sequence is 23.713 kD.

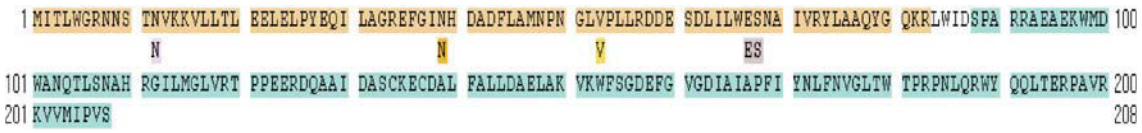

Figure 1-9: Protein sequence (primary structure) of YliJ indicating specific sequence features. The N-terminus domain residues are highlighted in yellow, while the C-terminus domain residues are highlighted in green. The predicted important catalytic residues asparagines 12 and 39, valine 53, glutamate 67, and serine 68 are indicated in purple and yellow colors.
Retrieved from http://www.uniprot.org/uniprot/P0ACA7

The hydropathy index plot (Figure 1-10) of YliJ sequence indicated that the protein is hydrophilic with a grand average of hydropathy (GRAVY) of -0.198. There are 22 cationic side chain residues (fourteen arginines, eight lysines, and two histidines), 28 anionic side chain residues (thirteen aspartates and fifteen glutamates) and a C-terminus carboxyl group[45, 46].

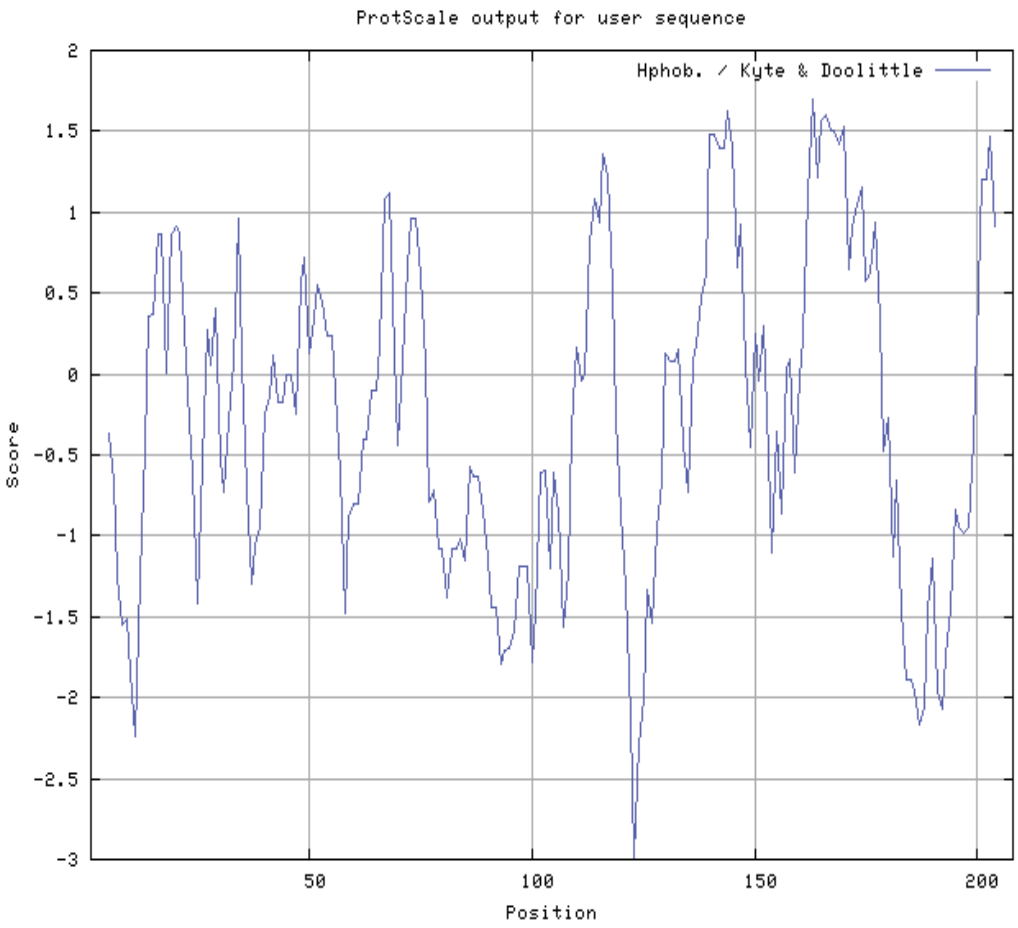

Figure 1-10: The hydropathy index plot of YliJ protein sequence using the

Kyte and Doolitte Hydropathicity scaling method of amino acids. Values below 0 indicate hydrophilic regions on the protein sequence of YliJ while peaks above 0 indicate hydrophobic regions of the protein sequence.

Elements of Predicted YliJ Secondary Structure

The secondary structure showed 54.3% alpha helices, 7.2% beta strands, and 38.5% of neither alpha nor beta strand. There are four beta strands in which the neighboring hydrogen-bonded polypeptide chains between strand 3 and the others are antiparallel (Figure 1-11).

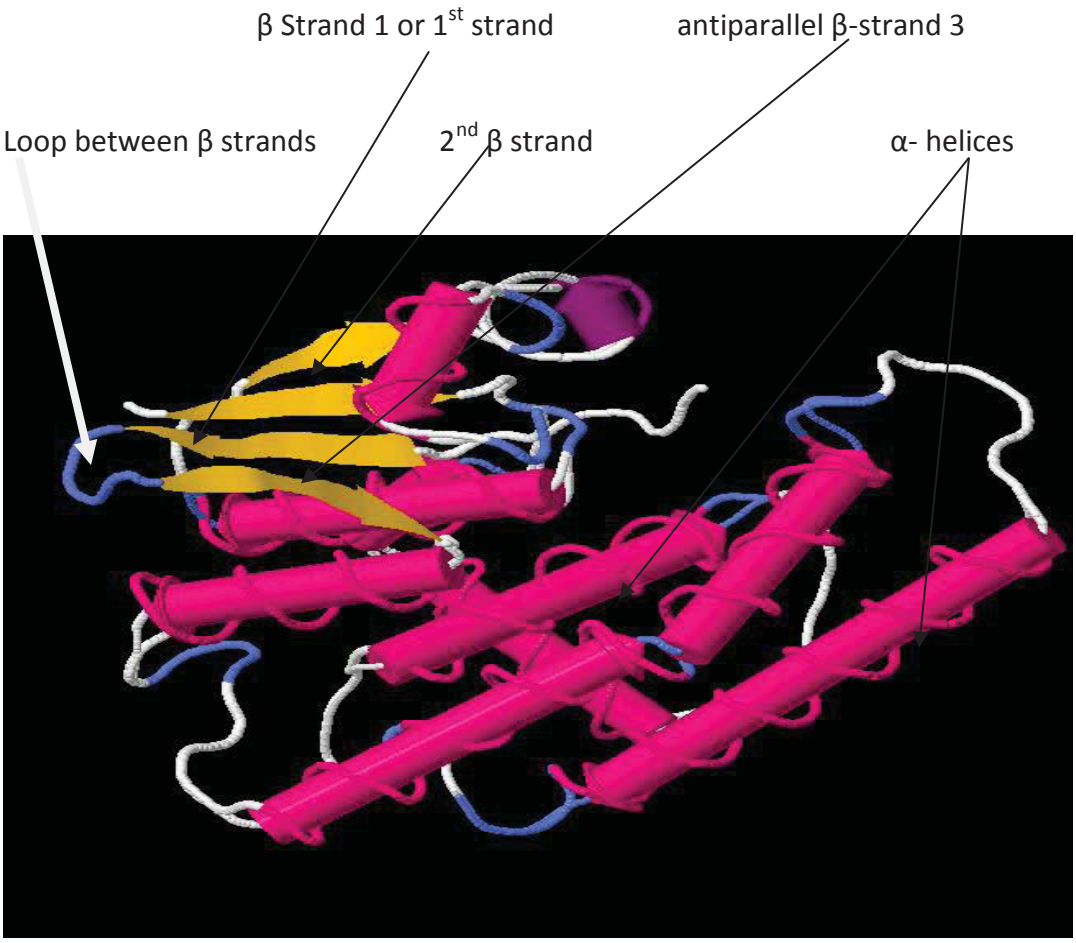

Figure 1-11: *Predicted secondary structure of YliJ. Alpha helices are shown as rockets while the four beta strands are shown as planks with arrowheads pointing towards the carboxy terminus. The directions of the arrows show that strand 3 is antiparallel to the others.*

The protein structure consists of two domains: the N-terminal and the C-terminal domains. The N-terminal domain is predicted to be conserved whereas the C-terminal domain is extremely variable. Based on their primary functions, N- and C-terminal domains are often referred to as the GSH (G-site) and xenobiotic substrate (H-site) binding domains, respectively[47].

The N-terminal domain exhibiting the thioredoxin fold is formed by about one third of the polypeptide chain with 83 amino acid residues (residues 1-83). Just like all cytosolic glutathione transferases, the thioredoxin fold of YliJ consists of a β-α-β-α-β-β-α structural motif which forms a varied four-strand beta sheet in the order of 4-3-1-2 as shown in Figure 1-11. The core of this domain is made up of three layers with the four beta strands sandwiched between α-helices (α/β/α)[47] (Figure 1-12). The N-terminal domain provides the binding site for glutathione.

The C-terminal domain which is formed by about two-thirds of the protein is an all α-helical domain with a unique protein fold. The core of this domain consists of a bundle of six helices (Figure 1-12). The C-terminal α-helical domain generally provides a binding site for the substrate (xenobiotic site). Usually, the xenobiotic moiety of the product is located in the crevice between the two domains and makes a number of contacts with residues in the C-terminal domain. In contrast, the glutathionyl portion of the product lies at the end of the β-sheet and interacts with the protein through a number of electrostatic interactions and hydrogen bonds[45-47].

Three-Dimensional Structure and Important Structural Features of YliJ

The spherical shape and solubility of YliJ makes it a globular protein (Figure 1-13). The polypeptide chain has seven sulfur atoms, five methionines and two cysteines but no disulfide bonds. Similar to most cytosolic GSTs, YliJ is proposed to have a dimeric

structure which stabilizes the tertiary structure of the individual subunits and presumably each of the two domains of the subunits[25].

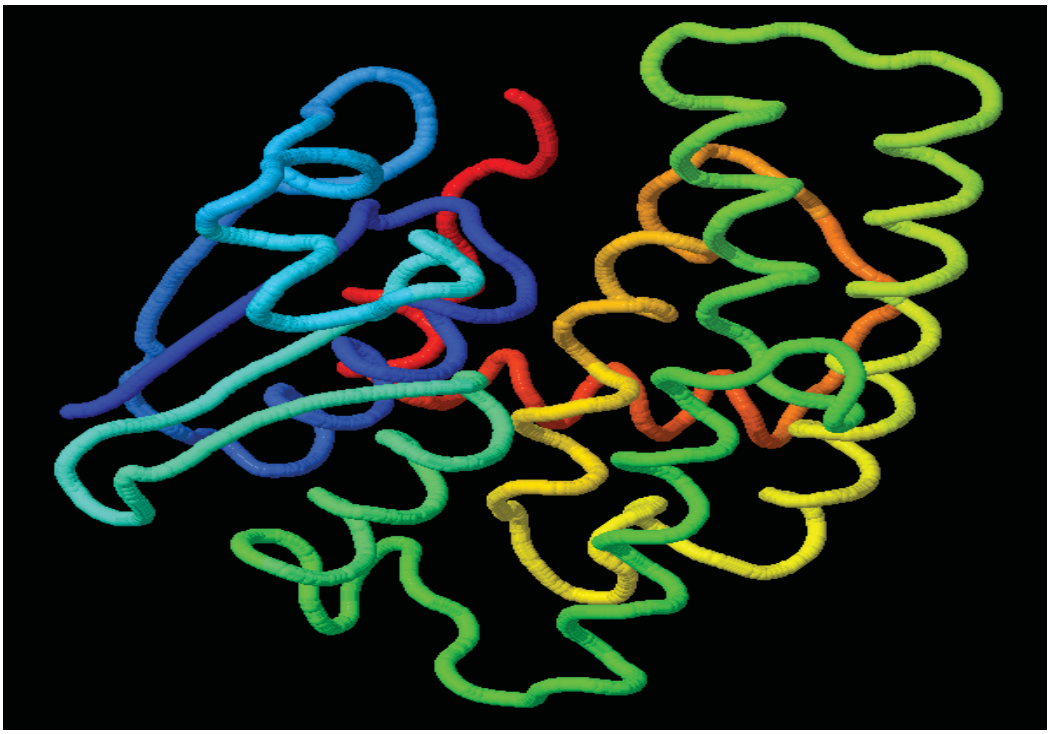

Figure 1-12: *Predicted 3-D structure of YliJ showing the spherical or folded shape that makes it a globular protein. N-terminus is shown in blue; C-terminus is shown in red. A GSH molecule is proposed to bind in a cleft between the N- and C-terminal domains.*

Based on the general catalytic functions of GSTs, YliJ is predicted to have sites to bind both GSH and the electrophilic moiety of a substrate at the enzyme's hydrophilic G-site (N-terminal domain) and the hydrophobic portion of a substrate at the H-site (C-terminal domain), respectively. Upon binding GSH, YliJ subsequently activates the sulfhydryl group of GSH to form a thiolate, enabling the nucleophilic attack on the

substrate[47]. The predicted catalytically important residues Asn-12, Asn-39, Val-53, Glu-67, and Ser-68, are located in the N-terminal domain (Figure 1-13). One of the three amino acid residues (Asn-12, Asn-39, or Val-53) is predicted to interact with the glycine residue of glutathione[49]. Specifically, hydrophobic valine-53 is imbedded in the interior of the protein where it participates in glutathione interaction through the amide nitrogen and carbonyl oxygen. The GSH binding site amino acid residues (Glu-67 and Ser-68) are located on the surface of the protein and in a close proximity to each other. This is suggested to facilitate the binding of GSH and subsequently the electrophilic substrate. Based on the predicted structure, YliJ appears to utilize the hydroxyl group of Ser-68 residue to activate the sulfhydryl group of bound GSH which then nucleophilically attacks the substrate[47]. Although, the hydrophobic H-site is proposed to be the binding site for the substrate, the catalytically important amino acid residues present in that site are not known and have yet to be experimentally determined.

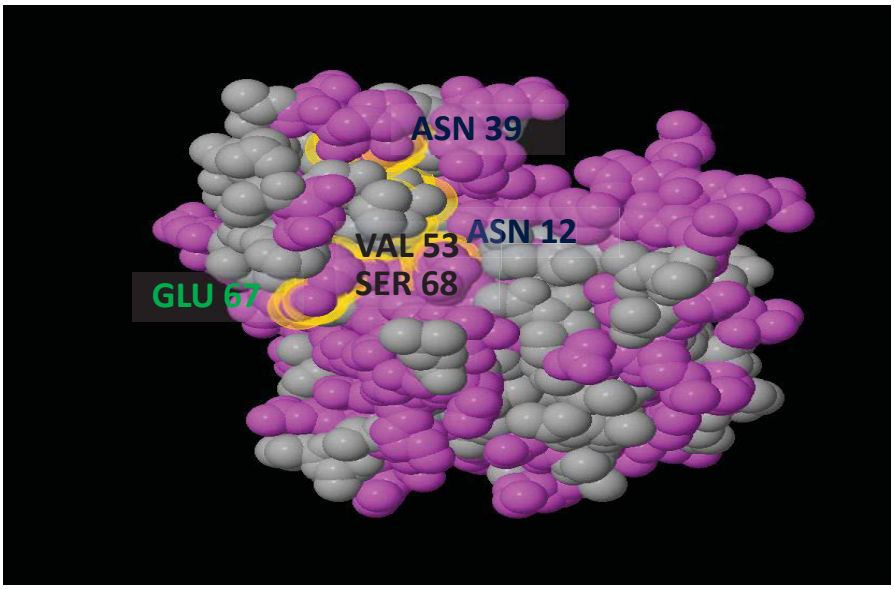

Figure 1-13: *Polar (charged and uncharged) and hydrophobic amino acid residues of YliJ. The purple color represents the polar or hydrophilic amino acids while the grey color represents hydrophobic amino acids. The amino acid residues important for YliJ function include four hydrophilic residues (Asn-12, Asn-39, Glu-67, and Ser-68) and one hydrophobic residue (Val 53). The residues responsible for GSH binding (Glu-67 and Ser-68) are located on the surface of the protein.*

Statement of Purpose

The goal of this research is to develop a simple purification procedure for YliJ, design a safe method for assaying YliJ activity, characterize YliJ, and to search for other potential substrates for YliJ. The YliJ protein has been postulated to play a key role in conferring resistance to halogenated compounds like bromoacetate.

YliJ will be overexpressed in *E. coli* cells and purified employing ammonium sulfate precipitation, and ion-exchange chromatography. The presence and purity of YliJ in a sample can be verified by sodium dodecyl sulfate-polyacrylamide gel electrophoresis (SDS-PAGE). The kinetic parameters of YliJ as it catalyzes the conjugation of bromoacetate or iodoacetate to glutathione (GSH) will then be determined.

In addition, the effect of temperature on YliJ stability and the effect of pH on YliJ activity will be determined. The sensitivity of *E. coli* cells to antibiotics and halogenated compounds will also be studied.

Chapter 2: Materials and Methods

Materials

L-Glutathione reduced, dithiothreitol (DTT), 5, 5'-dithio-bis (2-nitrobenzoic acid) (DTNB) were purchased from Sigma Aldrich (St. Louis, MO). Bromoacetic acid, iodoacetic acid, and iodoacetamide were purchased from Acros Organics (Belgium, WI). Ammonium sulfate, IPTG, Tris buffer, tetramethylethylenediamine (TEMED), sodium phosphate monobasic anhydrous, sodium acetate anhydrate, sodium dodecyl sulfate, MES free acid monohydrate, glycine, streptomycin sulfate, kanamycin, ampicillin, chloramphenicol, ethylenediaminetetraacetic acid (EDTA), EZ-vision loading dye, Luria-Bertani medium (LB broth), bacteriological agar were purchased from Amresco (Solon, Ohio). SOC medium was prepared from SOB broth, purchased from Amresco (Solon, Ohio), and 20% sterile glucose purchased from Amresco (Solon, Ohio). Protein molecular weight markers were purchased from Amresco and Bio-Rad (Hercules, California). Q-Sepharose Fast Flow was purchased from Amersham Biosciences (Pittsburgh, PA). Amicon ultra centrifugal filters were used for the protein concentration. HP Agilent 8453 Diode array spectrophotometer (Santa Clara, CA) was used for kinetic analysis. BL21 (DE3) was purchased from Invitrogen (Carlsbad, CA). Expression vector pET20b-*yliJ* and *E. coli* cells BW25113Δ*yliJ* were provided by Dr. Stourman.

Methods

Transformation and Expression of YliJ

All the Luria-Bertani (LB) media and LB-agar plates contained 100 µg/mL of ampicillin. 50 µL of BL21 (DE3) *E. coli* competent cells were thawed on ice. 2 µl of pET20-*ylij* plasmid DNA was added to the cells and incubated on ice for 30 minutes. The mixture was heat shocked for 45 seconds at 42 ^{o}C and left on ice for 5 minutes. 950 µl of SOC was pipetted into the mixture and the tube was shaken at 200 rpm for 60 minutes at 37 ^{o}C. 100 µL of the mixture was spread onto a LB agar plate and incubated overnight at 37 ^{o}C. A single colony of BL21 (DE3) cells containing pET20-*ylij* were used to inoculate 2 mL of LB media. The culture was incubated overnight at 37 ^{o}C with shaking at 150 rpm. The colony which gave the best protein expression was selected and used to inoculate 100 mL LB medium. The culture was incubated overnight at 37 ^{o}C with shaking at 150 rpm. 12 mL of the overnight culture was diluted into 1.2 L of LB media. The diluted culture (three flasks containing 1.2 L of culture in each) were grown on a shaker at 37°C until an OD_{600} of 0.6 was reached, indicating the exponential phase of cell growth. Once the cells reached an OD_{600} of 0.6, protein expression was induced by the addition of isopropyl-β-D-thio-galactoside (IPTG) to a final concentration of 0.3 mM. The cell culture was grown overnight at 37 ^{o}C with shaking at 200 rpm. The cells were then harvested by centrifugation at 6,000 x g at 4 ^{o}C for 10 minutes. The cell pellets were stored at -20 ^{o}C.

Streptomycin Sulfate Treatment and Ammonium Sulfate Precipitation

The cell pellets were resuspended in 10 mM Tris buffer, pH 7.0 with 2 mM EDTA and 1 mM DTT, and stirred on ice for one hour. The redissolved pellets were sonicated for a total of six cycles with 30 seconds of sonication and 1 minute cooling on ice between cycles to lyse the cells. The lysates were centrifuged at 11,000 × g at 4 ^{o}C for 30 minutes. The supernatant was treated with 1% (w/v) of streptomycin added dropwise as a solution of streptomycin sulfate in the same buffer. The solution was stirred for 20 minutes on ice and then centrifuged for 30 minutes at 11, 000 x g. Ammonium sulfate was added to the supernatant to 40% saturation. The solution was stirred on ice for 20 minutes and was centrifuged for 30 minutes at 11, 000 x g. The pellet was stored at 4 ^{o}C. The supernatant was brought to 75% saturation by adding more ammonium sulfate. The mixture was then centrifuged at 11,000 x g for 25 minutes after 10 minutes of stirring on ice. The pellet was stored at 4 ^{o}C. 20 µL of the supernatant after each centrifugation step as well as small amount of the pellet resulting from ammonium sulfate precipitation were dissolved in 10 mM Tris buffer, pH 7.0 containing 2 mM EDTA. Each sample was mixed with 2x SDS loading buffer in a 1:1 ratio, heated at 100 ^{o}C for 5 minutes, and analyzed using 12% SDS-PAGE at 200 V. The results obtained from the SDS-PAGE analysis were used as the basis for further purification of YliJ.

Dialysis of 40% and 75% Pellets

The 40% and 75% ammonium sulfate pellets were dissolved in 10 mL and 5 mL of 20 mM sodium phosphate buffer, pH 6.5 containing 1 mM DTT, respectively. The redissolved pellets were placed in a dialysis bag and suspended in a 2 L flask with 20 mM sodium phosphate buffer, pH 6.5. The flask was placed on a stirrer overnight at 4 ^{o}C.

Protein Purification by Ion Exchange Chromatography

The ion exchange column employed in this purification process was the Q-Sepharose Fast Flow. All protein solutions were stored at 4 °C for short term and at -20 ^{o}C for long term.

The Q-Sepharose Fast Flow column (3 x 12 cm) was equilibrated with 500 mL of 20 mM sodium phosphate buffer, pH 6.5, containing 1 mM DTT. The dialyzed protein samples from both the 40% and 75% ammonium sulfate precipitation were combined and centrifuged at 4 °C for 10 minutes at 5,000 × g. The supernatant was gently loaded onto the column via a pipette without disturbing the column. The flow through was collected. The column was washed with 500 mL of 20 mM sodium phosphate buffer, pH 6.5, containing 1 mM DTT to remove unbound proteins. The proteins retained by the column were eluted with a gradient of 0-400 mM NaCl in 20 mM sodium phosphate, pH 6.5 and 3 mL fractions were collected. Following the elution of proteins from the column, the absorbance at 280 nm of each fraction was measured, and the fractions with the highest absorbance were analyzed by SDS-PAGE.

SDS-PAGE Analysis and Concentration of Protein Samples

20 µL of each fraction from the ion exchange column that showed significant absorbance at 280 nm was mixed with 20 µL of protein loading dye. The mixture was heated at 100 ^{o}C for 5 minutes and centrifuged for about 30 seconds. A standard molecular weight protein marker and each sample were loaded on a sodium dodecyl sulfate polyacrylamide gel with a 12.5% resolving gel and 4.5% stacking gel. The gel was run for 35 minutes at 200 V using SDS buffer and then stained with Coomassie blue stain for 30 minutes on a shaker. This was followed by 60 minutes destaining on a shaker with protein destaining buffer. The samples which gave clear intense bands at 23 kDa on the SDS-PAGE were pooled together and concentrated using Amicon Ultra-4 centrifugal unit (10,000, MWCO). The concentration of YliJ was determined from absorbance at 280 nm using extinction coefficient of 51450 $M^{-1}cm^{-1}$.

Analysis of YliJ Kinetics

YliJ activity was assayed in the reaction of GSH and bromoacetate. The amount of GSH in the solutions was quantified using 5, 5'-dithio-bis-(2-nitrobenzoic acid) (DTNB). The molar absorption coefficient (εM) of TNB at 412 nm is 13600 M^{-1} cm^{-1}. All enzyme reactions were conducted at room temperature (25 ^{o}C). The pH of the stock solutions of GSH and bromoacetate was adjusted to 7.0 before they were added to the reactions. YliJ activity was determined by varying the concentration of GSH while holding the amount of bromoacetate constant. Final concentrations of GSH varied from 0.157 mM

to 10 mM. Three different sets of reaction tests were conducted for each of the seven different concentrations of GSH. The first set of reactions (control) tubes contained 450 µL of 150 mM sodium phosphate buffer, pH 7.0 and 50 µL of corresponding GSH solution. The second set of reactions (uncatalyzed reactions) contained 360 µL of sodium phosphate buffer, (150 mM, pH 7.0), 90 µL of bromoacetate, pH 8.0, and 50 µL of corresponding GSH solution. The third set of reactions (catalyzed reactions) contained 350 µL of sodium phosphate buffer (150 mM, pH 7.0), 50 µL of corresponding GSH solution, 10 µL of purified YliJ protein (0.8 µM stock protein solution) and 90 µL of bromoacetate (58 mM, pH 7.0). Each reaction was allowed to proceed for 3 minutes at room temperature then 25 µL of reaction mixture were added to a spectrophotometric cuvette which already contained 950 µL of Tris buffer (200 mM, pH 8.0) and 25 µL of 5 mM DTNB. The absorbance of the solution was measured at 412 nm. Assays were duplicated and the results were averaged for each concentration of GSH used. The rate of each reaction was calculated using the extinction coefficient of TNB. For each concentration of GSH, the rate of YliJ-catalyzed reaction was determined as a difference between the rates of catalyzed and uncatalyzed reactions. The kinetic parameters V_{max}, K_M and k_{cat} were calculated from the plot of initial velocity against concentration of GSH. The experiment was also repeated replacing bromoacetate with iodoacetate as substrate. A Lineweaver-Burk plot was generated for YliJ catalyzed conjugation of GSH and iodoacetate and the kinetic parameters V_{max}, K_M, and k_{cat} were determined.

Thermal Stability of YliJ Protein

The thermal stability of the purified YliJ was evaluated by incubating the protein for 5 min at various temperatures from 25 ^{o}C to 60 ^{o}C. The samples after incubation were cooled down, centrifuged for about 1 minute, and 10 µL was pipetted into an assay mixture of 50 µL GSH (30 mM, pH 7.0), 350 µL sodium phosphate buffer (150 mM, pH 7.0) and 90 µL of bromoacetate (58 mM, pH 7.0). The reaction was allowed to proceed for 3 minutes. 25 µL of this reaction mixture was added to an assay cocktail containing 950 µL Tris buffer (200 mM, pH 8.0) and 25 µL DTNB (5 mM) and the absorbance was taken at 412 nm. The rate of YliJ activity was then determined for each temperature.

Effect of pH on YliJ Activity

The pH stability of YliJ protein was determined at room temperature using different buffers within the pH range of 5.0 to 9.0. The buffers used were 100 mM concentration sodium acetate buffer (pH 5.0), MES buffer (pH 6.0), sodium phosphate buffer (pH 7.0), Tris buffer (pH 8.0, 9.0). 30 mM GSH solutions were prepared in the same buffers. The reaction mixtures contained 350 µL of the buffer solution, 50 µL of the corresponding GSH solution, 10 µL YliJ protein (0.8 µM), and 90 µL of bromoacetate solution (58 mM). The reaction was allowed to proceed for 3 minutes. 25 µL of this reaction mixture was added to an assay cocktail containing 950 µL Tris buffer (200 mM, pH 8.0) and 25 µL DTNB (5 mM) and the absorbance was taken at 412 nm. The rate of YliJ activity was then determined for each pH.

Testing the Sensitivity to Halogenated Compounds

The sensitivity of wild type and knockout strains of *E. coli* to selected halogenated compounds was determined using the agar disc diffusion test. Different concentrations (100 mM, 50 mM, 10 mM and 2 mM) of bromoacetate, iodoacetate, and iodoacetamide were used. Cultures of wild type (*E. coli* cells expressing YliJ protein) and knockout strain BW25113Δ*ylij* lacking YliJ were grown overnight in LB medium on shaker at 37 ^{o}C. 200 µL of the grown cells were plated on LB agar medium which did not contain antibiotics and 0.6 cm discs cut out of filter paper were placed on the plates. 5 µL of each chemical solution was pipetted onto the center of the discs. The plates were incubated overnight at 37 ^{o}C. The sensitivity of the cells to chemicals was evaluated by measuring the diameter of bacterial clearance around the disc.

Testing for Antibiotic Sensitivity

The antibiotics used were ampicillin, chloramphenicol, and fosfomycin. The final concentrations ranged from 0.2 mg/mL to 10 mg/mL for ampicillin; 0.1 mg/mL to 5 mg/mL for fosfomycin; 0.06 mg/mL to 3 mg/mL for chloramphenicol. Cultures of *E. coli* cells expressing YliJ protein and knockout strain lacking YliJ were grown on a shaker overnight at 37 ^{o}C and 200 µL of the overnight growth were plated on LB agar medium which did not contain antibiotics. 0.6 cm discs cut out of filter paper were placed on the plates and 5 µL of antibiotic solution was pipetted onto the center of the discs. The

plates were then incubated overnight at 37 ^{o}C. Sensitivity of the cells was determined by measuring the diameter of growth inhibition around the discs.

CHAPTER 3: RESULTS

Expression of YliJ Proteins

Expression of YliJ protein was examined in seven colonies of BL21 (DE3) cells containing pET20-*ylij*. The *E. coli* cells after transformation with pET20-*ylij* were plated on LB medium containing ampicillin and incubated overnight. Seven different colonies were picked from the plate after overnight incubation to prepare liquid cultures. Each culture was incubated overnight at 37 ^{o}C with shaking at 150 rpm. Figure 3-1 represents the SDS-PAGE analysis of protein expression before (lanes 1a-7a) and after induction with IPTG (lanes 1b-7b). Addition of IPTG induces the expression of YliJ protein which is indicated by the increased intensity of the bands near 23 kDa (lanes 1b to 7b).

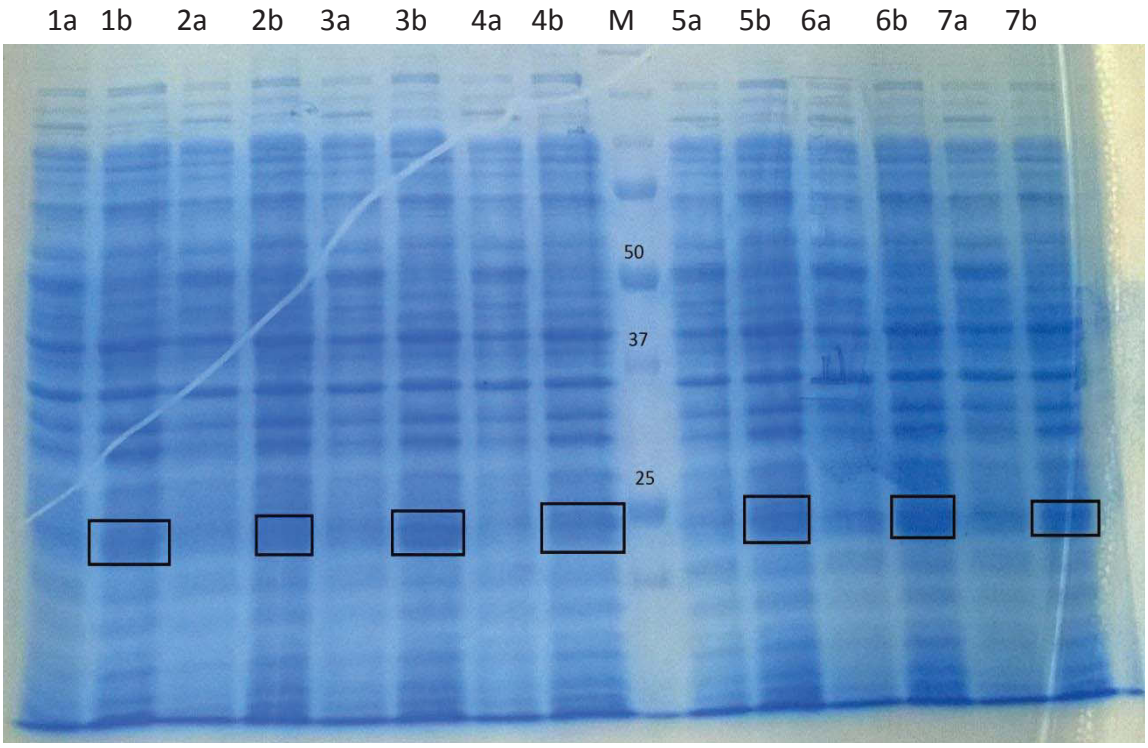

Figure 3-1: SDS-PAGE of pET20-*ylij* transformed into BL21 (DE3) cells before and after IPTG induction. Lanes 1a-7a: BL21 (DE3) cells containing pET20-*ylij* before IPTG induction; Lanes 1b-7b: BL21 (DE3) cells containing pET20-*ylij* induced with IPTG. Lane M: protein molecular weight marker.

Streptomycin Sulfate Treatment and Ammonium Sulfate Precipitation

Initial purification of YliJ from *Escherichia coli* involved cell lysis by sonication, treatment with streptomycin, and ammonium sulfate precipitation. Samples at each step of purification were analyzed by SDS-PAGE (Figure 3-2). The *E. coli* BL21 (DE3)-*ylij* cells were harvested by centrifugation and the cell pellets were resuspended in 10 mM Tris buffer, pH 7.0 with 2 mM EDTA and 1 mM DTT, and then sonicated to lyse the cells.

The supernatant after sonication (Figure 3-2, Lane 3) was treated with 1% (w/v) of streptomycin sulfate to precipitate DNA. The mixture after streptomycin treatment was centrifuged to collect the precipitated DNA as the pellets (Lane 4), leaving YliJ to remain in the solution (Lane 5). The supernatant was treated with ammonium sulfate to 40 % saturation. Lane 6 shows a band near 23 kDa in the pellets after 40 % ammonium sulfate precipitation. Proteins remaining in the supernatant (Lane 7) were further precipitated at 75% ammonium sulfate saturation. The intense bands for YliJ are shown in lanes 6, 7, 9, and 10. The pellets obtained after ammonium sulfate precipitation were used for further purification.

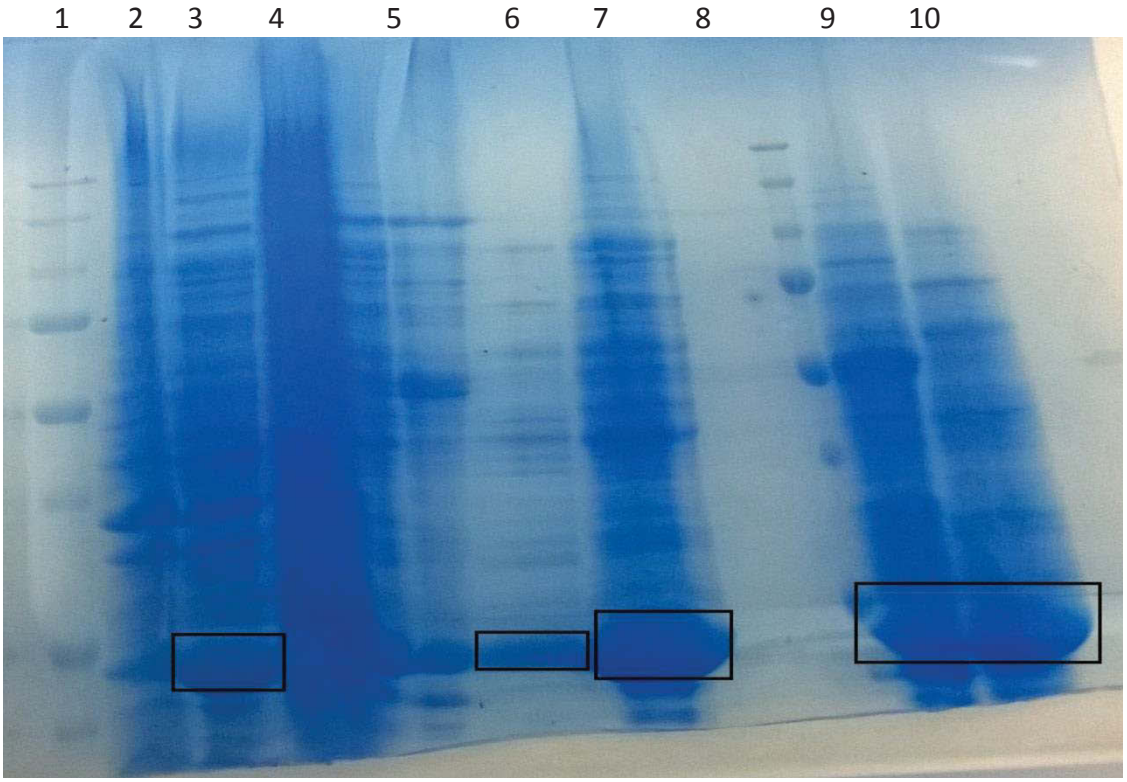

Figure 3-2: SDS-PAGE of fractions from the initial purification of the YliJ protein. Lane 1: protein molecular weight marker; Lane 2: pellet after sonication; Lane 3: supernatant after sonication; Lane 4: pellet after streptomycin treatment; Lane 5: supernatant after streptomycin treatment; Lane 6: pellet after 40 % ammonium sulfate precipitation; Lane 7: supernatant after 40 % ammonium sulfate precipitation; Lane 8: protein molecular weight marker; Lane 9: pellet after 75 % ammonium sulfate precipitation; Lane 10: supernatant after 75 % ammonium sulfate precipitation.

Protein Purification by Ion Exchange Chromatography

The Fast Flow Q Sepharose ion exchange column was used to further purify the protein after the ammonium sulfate precipitation. The pellets obtained from the 40%

and 75% saturation of ammonium sulfate were combined, resuspended in 20 mM sodium phosphate buffer, pH 6.5, and dialyzed overnight against the same buffer at 4 ^{o}C. The dialyzed sample was centrifuged and loaded onto the Q Sepharose Fast Flow column. The proteins retained by the column were eluted with a gradient of 0-400 mM NaCl in 20 mM sodium phosphate, pH 6.5. The absorbance at 280 nm was taken for all the eluted fractions. The fractions which showed significant absorbance at 280 nm were then analyzed using SDS-PAGE (Figure 3-3). The band for YliJ is clearly visible in lanes 2-12. The fractions collected from the Q Sepharose Fast Flow column that contained most YliJ protein were then combined and concentrated.

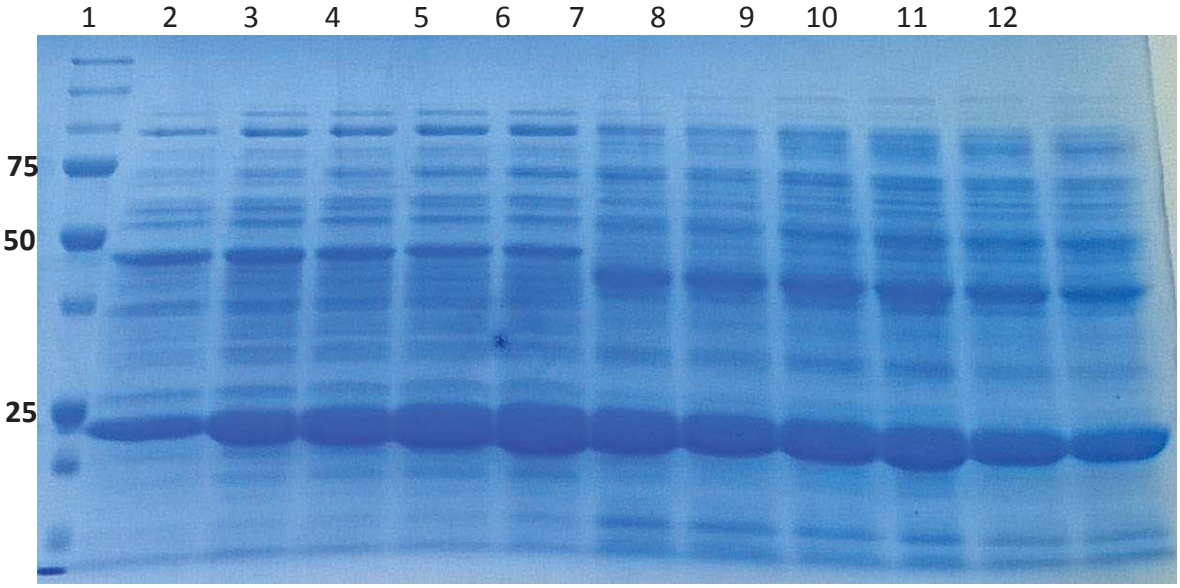

Figure 3-3: SDS-PAGE of fractions from ion exchange chromatography. Lane 1: protein molecular weight marker; Lane 2: load; Lane 3-12: Fractions collected during elution with linear gradient of (0-400 mM) NaCl in 20 mM sodium phosphate buffer that showed high absorbance at 280 nm.

The 10, 000 MWCO Amicon Ultra-4 centrifugal unit was used to concentrate the pooled fractions. Figure 3-4 shows the SDS-PAGE analysis of the 10K concentrated fractions. Lane 3 (10K concentrated supernatant) shows a nearly pure fraction of YliJ as intense band near 23 kDa. The protein concentration was determined from the absorbance at 280 nm and the extinction coefficient of 51450 $M^{-1}cm^{-1}$.

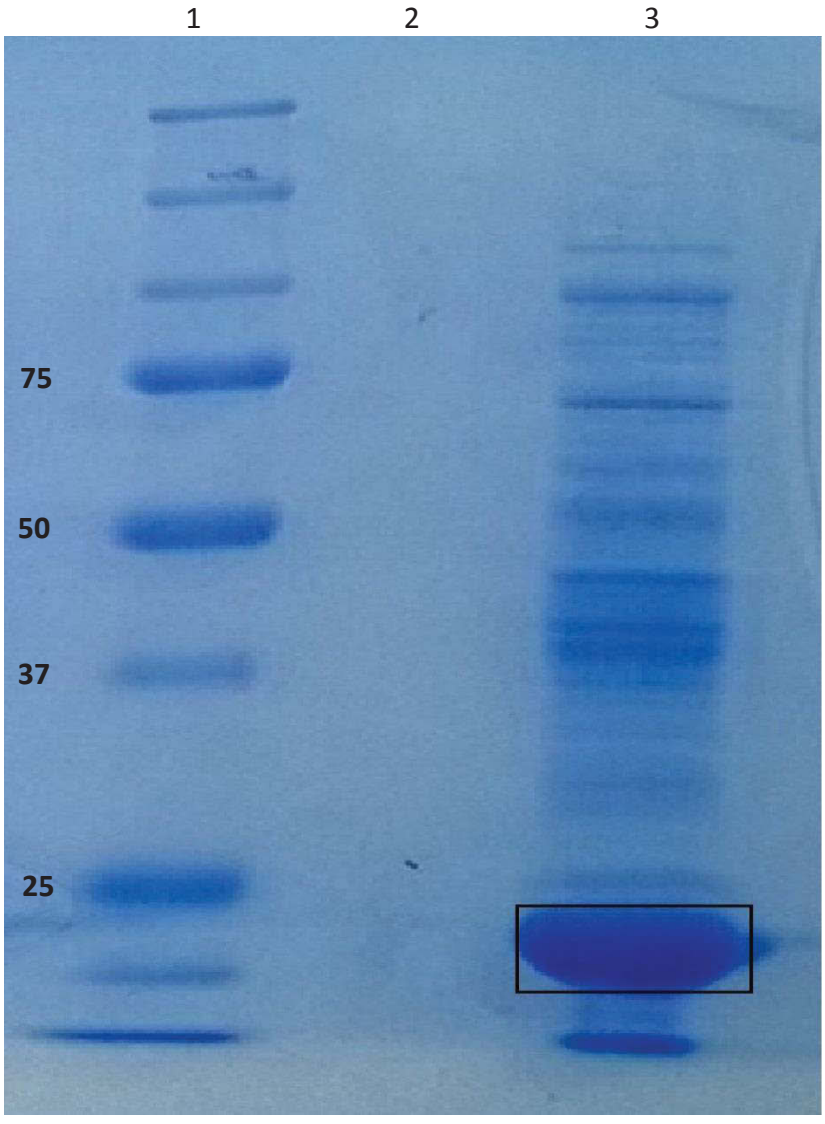

Figure 3-4: SDS-PAGE of concentrated YliJ. Protein marker (Lane 1), 10K flow through fraction (Lane 2), 10K concentrated supernatant fraction (Lane 3).

Analysis of YliJ Kinetics

The purified protein sample was used to determine the kinetic parameters of YliJ. YliJ activity was determined by varying the concentration of GSH while maintaining the amount of bromoacetate constant. Concentrations of GSH varied from 0.157 mM to 10 mM. Three separate reactions were prepared for each experiment (control, uncatalyzed, and catalyzed). The control contained the sodium phosphate buffer and the GSH solution and was used to accurately determine initial concentrations of GSH. The uncatalyzed reaction was initiated by adding bromoacetate to a mixture of sodium phosphate buffer and GSH solution. This was done because GSH can react with bromoacetate in the absence of the enzyme. For the catalyzed reaction, the reaction was initiated by adding bromoacetate to a mixture of YliJ sample (0.016 µM), GSH and buffer solution. The reactions were run at room temperature for 3 minutes. The amount of GSH that remained in the solution was quantified using 5,5'-dithio-bis-(2-nitrobenzoic acid) (DTNB). For each concentration of GSH, the assay was repeated twice and the rates of the reaction were averaged. The molar absorption coefficient (εM) of TNB at 412 nm is 13600 M^{-1} cm^{-1}. The initial velocity of YliJ was calculated as a function of change in concentration of GSH per unit time using Equation 1. The dilution factor used was 100 as shown in the equation.

$$\text{Initial velocity} = \frac{\mu mol}{sec} = \frac{A(412\text{ nm})}{13600\ M^{-1}} \times \frac{10^6\ \mu M}{M} \times 100 \times \frac{1}{3\ min} \times \frac{1\ min}{60\ sec} \qquad \text{(Equation 1)}$$

The experiment was also repeated replacing bromoacetate with iodoacetate as a substrate.

A plot of initial velocity against concentration of GSH was generated (Figure 3-5). From Figure 3-5, the maximum velocity of the YliJ catalyzed reaction (V_{max}) and the Michaelis constant (K_M), were determined. Table 3-1 shows the kinetic parameters of YliJ protein. The turnover number (k_{cat}) is the number of substrate molecules that are converted to product by the enzyme per unit of time. The YliJ catalytic parameters, K_M and k_{cat} were determined to be 1.60 mM and 175 s^{-1} from the Michaelis-Menten plot of initial velocity vs. concentration of GSH (Figure 3-5). The catalytic efficiency (k_{cat}/K_M) was also calculated to be 1.09×10^5 M^{-1} s^{-1}. Following the same procedure, a Lineweaver-Burk plot was generated for the reaction of YliJ, GSH, and iodoacetate (Figure 3-6). The kinetic parameters were also determined for the YliJ catalyzed reaction between GSH and iodoacetate (Table 3-1).

Table 3-1: Kinetic Parameters of YliJ

Enzyme	**Substrate**	**V_{max}** ($\mu M s^{-1}$)	**K_M** (mM)	**k_{cat}** (s^{-1})	**k_{cat}/K_M** ($M^{-1}s^{-1}$)
YliJ	Bromoacetate	2.80	1.60	175.0	1.09×10^5
YliJ	Iodoacetate	2.49	0.175	155.3	8.86×10^5

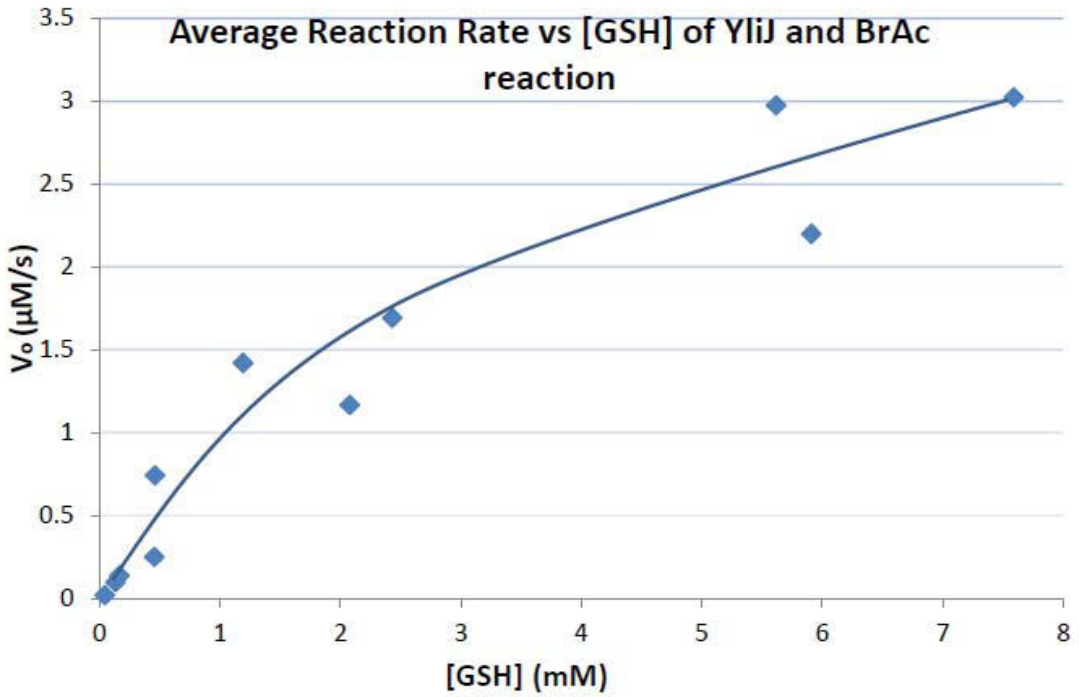

Figure 3-5: Plot of the reaction rate of YliJ catalyzed conjugation of glutathione (GSH) and bromoacetate (BrAc).

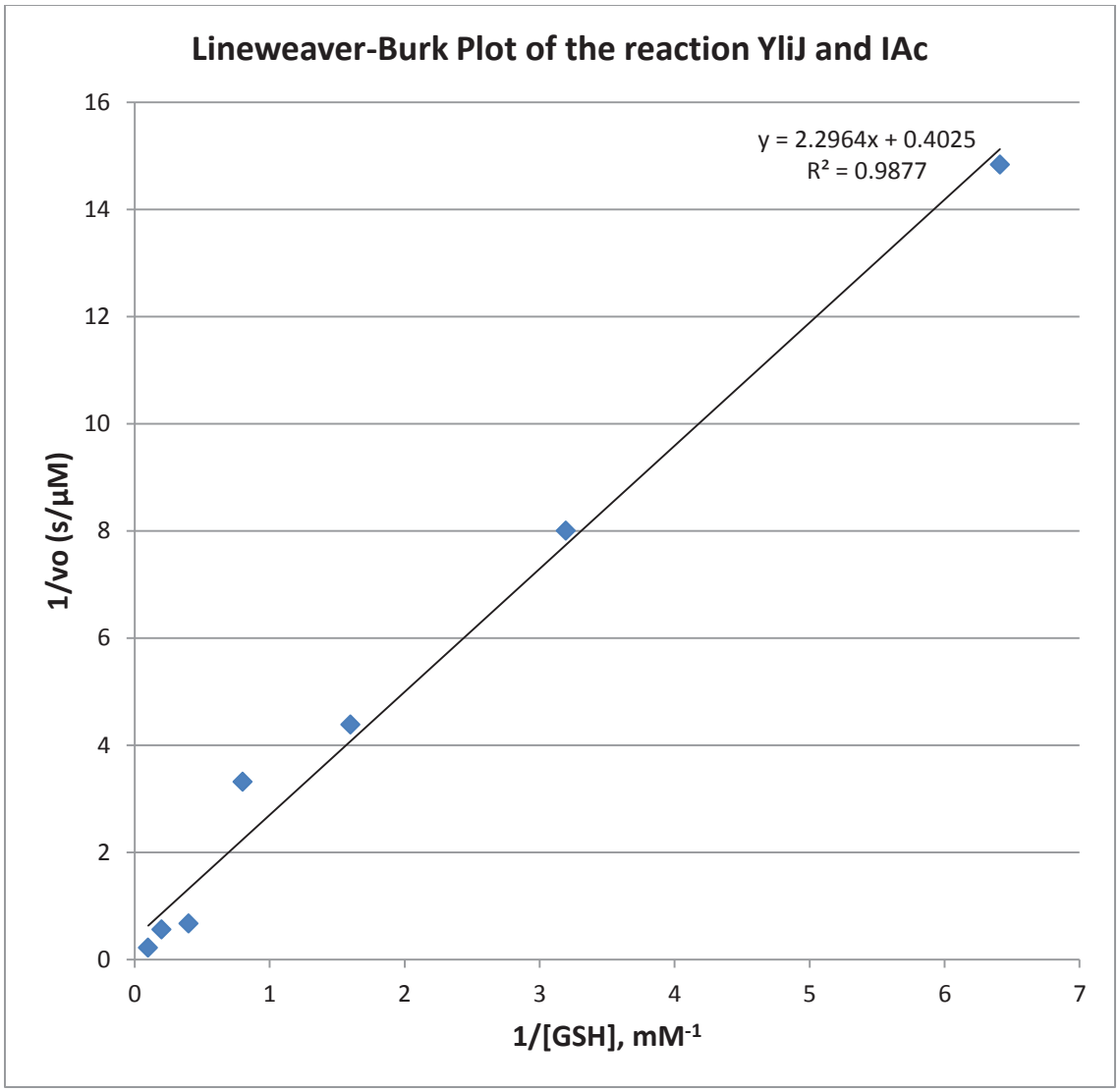

Figure 3-6: Lineweaver-Burk plot of the YliJ catalyzed reaction between GSH and iodoacetate (IAc).

Thermal Stability of YliJ Protein

The effect of temperature on the stability of the enzyme was studied. The thermostability of the YliJ protein was investigated by incubating the enzyme for 5 minutes at various temperatures from 25 ^{o}C to 60 ^{o}C and measuring the activity that remained after incubation of the protein at these temperatures. As shown in Figure 3-7, the activity after incubation of the enzyme at 25 ^{o}C was recorded as the highest YliJ activity (100% YliJ activity). The enzyme activity declined to 63% after incubation at 50°C and about 50% after incubation at 60°C.

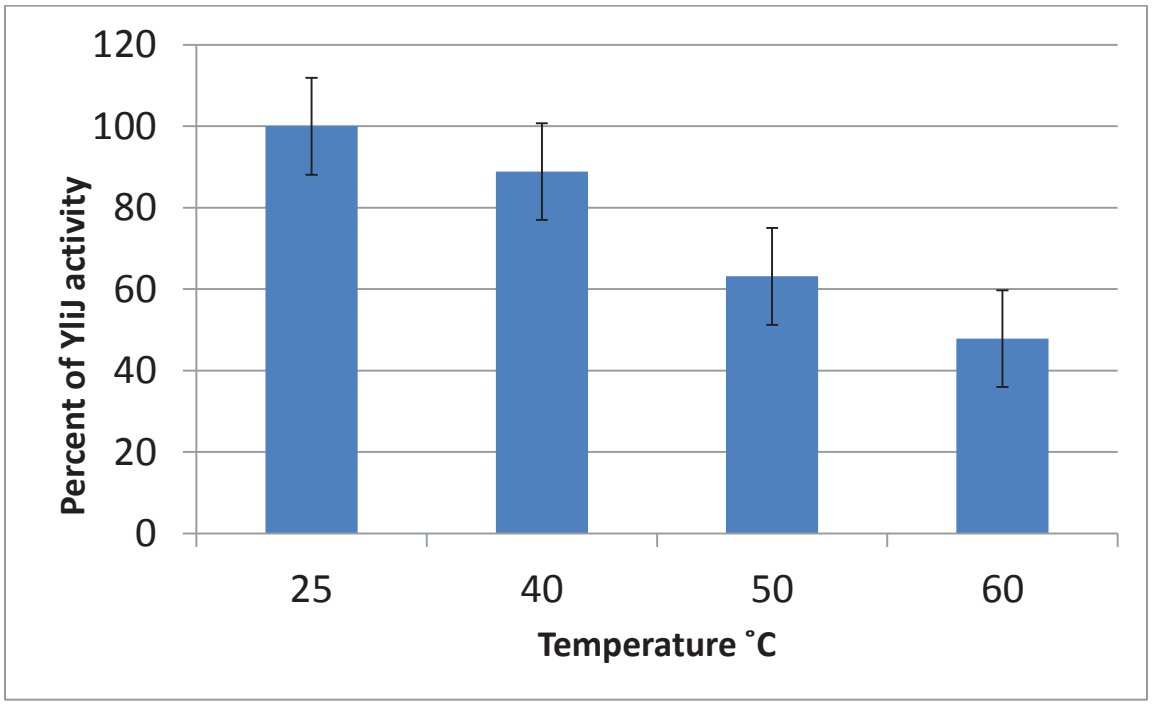

Figure 3-7: Effect of temperature on enzyme stability. Percent of YliJ activity remained after incubation of enzyme at different temperatures for 5 minutes. The enzyme activity at 25 ^{o}C was taken as 100%.

Effect of pH

The activity of an enzyme depends strongly on the pH of the assay mixture. The pH dependence of YliJ activity was determined at room temperature using different buffers within the pH range from 5.0 to 9.0. As shown in Figure 3-8, YliJ activity was detected at all five pH values tested (5.0, 6.0, 7.0, 8.0, and 9.0). The optimum pH for YliJ activity was found to be pH 7.0. At pH 5.0, the activity of YliJ was about 36% lower when compared to pH 7.0 (optimum pH). However, at a more basic solution (pH 9.0), the activity of YliJ was only 21 % lower when compared to the optimum pH.

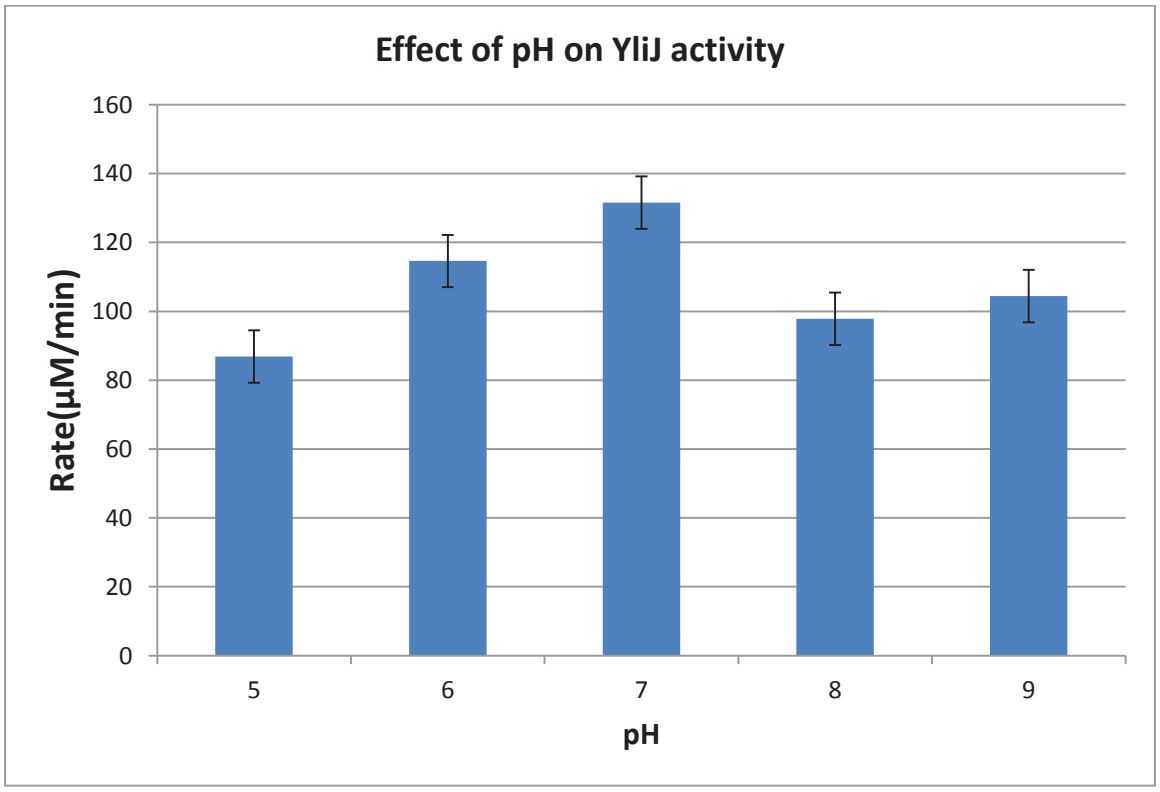

Figure 3-8: Effect of pH on enzyme activity. The activity of YliJ protein was measured at different pH's.

Testing the Sensitivity to Halogenated Compounds

The specificity of YliJ towards possible substrates was investigated by comparing the sensitivity of *yliJ* knockout and wild type *E. coli* strains to selected halogenated compounds. The agar disc diffusion test was conducted using different concentrations (2 mM-100 mM) of bromoacetate, iodoacetate, and iodoacetamide. Overnight cultures of wild type *E. coli* cells expressing YliJ protein and knockout strain BW25113Δ*yliJ* lacking YliJ were plated on LB agar plates. Different concentrations of chemicals were spotted on paper discs placed on the top of the inoculated plates. Sensitivity of the cells to the chemicals was evaluated by measuring the diameter of bacterial clearance around the disc after overnight incubation at 37 ^{o}C (Table 3-2). The wild type *E. coli* was more resistant to bromoacetate (BA) and iodoacetate (IA) than the *ylij*-knockout strain (Figure 3-9). The sensitivity of both the wild type and the knockout strains to iodoacetamide (IAA) was relatively high.

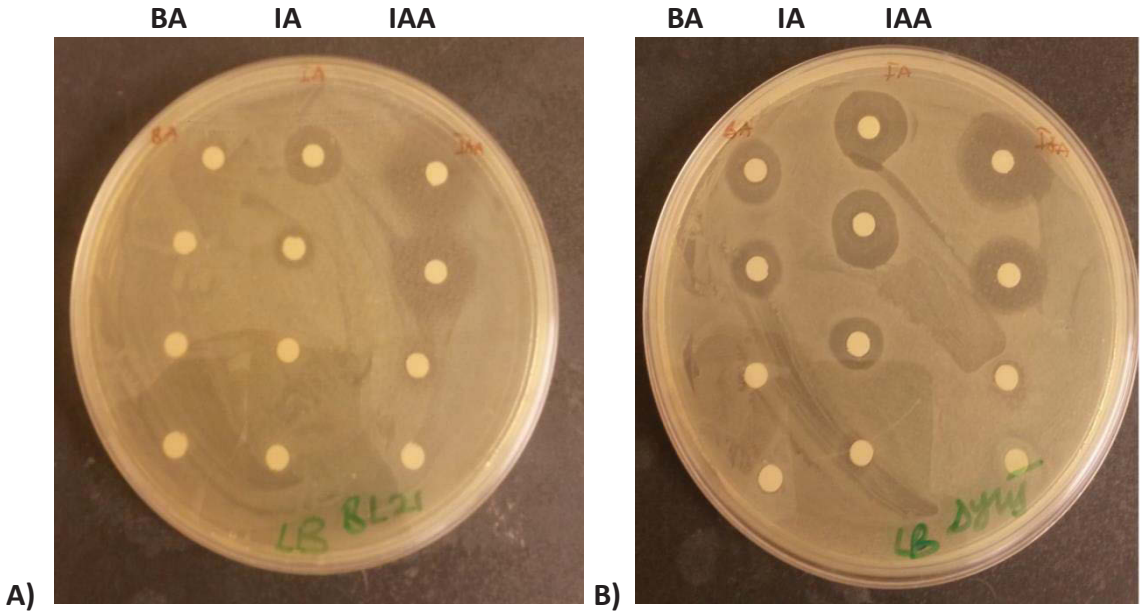

Figure 3-9: LB agar plates were used to determine the sensitivity of wild type and *yliJ*-knockout *E. coli* strains to halogenated compounds. Both the wild type *E. coli* cells (A) and knockout strain lacking YliJ (B) showed very high sensitivity towards iodoacetate (IA) and iodoacetamide (IAA). The knockout strain was more sensitive to bromoacetate (BA) than the wild type cells.

As shown in Table 3-2, iodoacetamide caused cell growth inhibition at all concentrations tested with the exception of the lowest concentration (2 mM) for both the wild type and knockout strains. For both *E. coli* strains, the inhibition of cell growth by iodoacetamide was higher compared to the other halogenated compounds. Iodoacetate showed some minor inhibition in the wild type cells but greater inhibition in the knockout strain. However, bromoacetate showed some inhibition in the knockout strain cells at high concentrations while the wild type strain showed complete resistance to all bromoacetate concentrations.

Table 3-2. Diameter of clearance (cm) of wild type *E. coli* and knockout *Δylij* strains grown on LB medium in the presence of selected halogenated compounds.

	Diameter of clearance (cm)			
Concentration of bromoacetate	**2.0 mM**	**10.0 mM**	**50.0 mM**	**100.0 mM**
Wild type *E. coli*	N/I	N/I	N/I	N/I
ΔyliJ-strain	N/I	N/I	1.2	1.5
Concentration of iodoacetate	**2.0 mM**	**10.0 mM**	**50.0 mM**	**100.0 mM**
Wild type *E. coli*	N/I	N/I	0.9	1.1
ΔyliJ-strain	N/I	1.4	1.8	2.1
Concentration of iodoacetamide	**2.0 mM**	**10.0 mM**	**50.0 mM**	**100.0 mM**
Wild type *E. coli*	N/I	0.9	2.1	2.5
ΔyliJ-strain	N/I	0.9	2.1	2.8

N/I indicates a field in which no growth inhibition was observed

Testing the Sensitivity to Antibiotics

The wild type and *ylij*-knockout *E. coli* strains were exposed to three different antibiotics: ampicillin (A), chloramphenicol (C) and fosfomycin (F) using the agar disc diffusion method of testing (Figure 3-10). Cultures of the *E. coli* wild type and *yliJ*-knockout strains were grown on LB media overnight at 37 ^{o}C, then plated on LB agar and exposed to various concentrations of antibiotics. As shown in Figure 3-10, the sensitivity of both the wild type *E. coli* cells (A) and the knockout strain (B) to fosfomycin was very high compared to ampicillin. Surprisingly, with chloramphenicol, the wild type cells were more sensitive than the knockout strain.

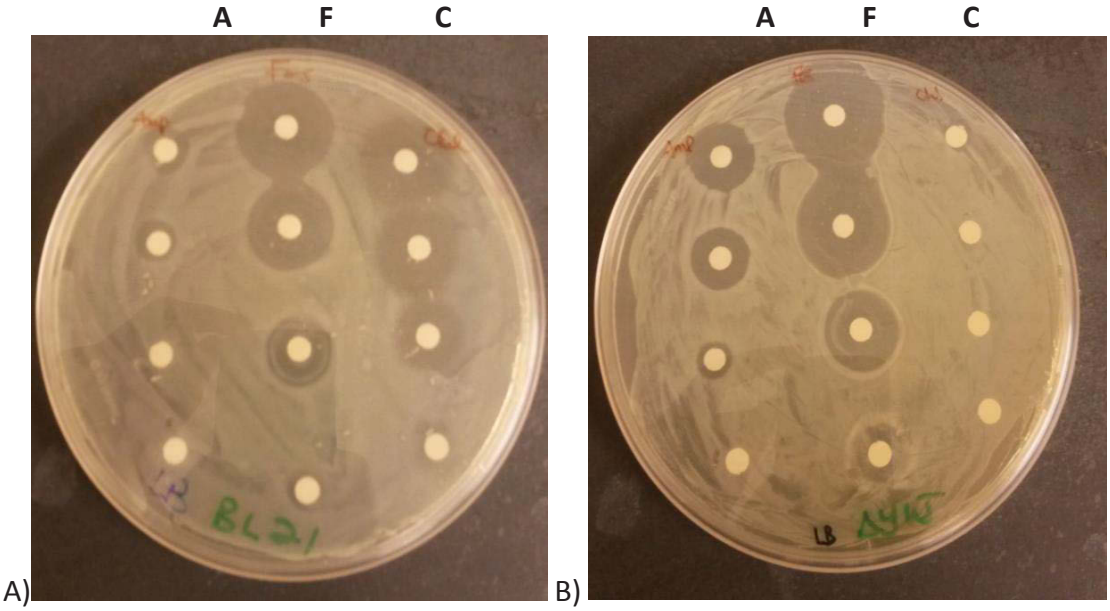

Figure 3-10: LB agar plates showing the sensitivity of *E.coli* strains to selected antibiotics. The wild type *E. coli* cells (A) and the knockout strain (B) both showed very high sensitivity to fosfomycin (F). With chloramphenicol (C), the wild type cells were more sensitive than the knockout strain.

The wild type *E. coli* strain showed little or no growth inhibition when exposed to different concentrations of ampicillin with 1.2 cm diameter of clearance at the highest concentration tested (Table 3-3). As indicated in Table 3-3, the knockout Δ*ylij* strain showed significant sensitivity to ampicillin where the diameter of growth inhibition was 2.0 cm at the highest concentration compare to 1.2 cm of the wild type *E. coli*. Both *E. coli* strains showed significant increase in growth inhibition when exposed to fosfomycin. The wild type cells showed an increased sensitivity to chloramphenicol but the knockout Δ*ylij* strain had no growth inhibition indicating an increase of resistance to the antibiotic.

Table 3-3. Diameter of clearance (cm) of wild type *E. coli* and knockout Δ*ylij* strains grown on LB medium in the presence of antibiotics.

	Diameter of clearance (cm)			
Concentration of ampicillin	**0.2 mg/mL**	**1.0 mg/mL**	**5.0 mg/mL**	**10 mg/mL**
Wild type *E. coli*	N/I	N/I	1.0	1.2
ΔyliJ-strain	N/I	0.9	1.7	2.0
Concentration of fosfomycin	**0.1 mg/mL**	**0.5 mg/mL**	**2.5 mg/mL**	**5.0 mg/mL**
Wild type *E. coli*	0.8	1.7	2.4	2.7
ΔyliJ-strain	1.2	2.3	2.9	3.1
Concentration of chloramphenicol	**0.06 mg/mL**	**0.3 mg/mL**	**1.5 mg/mL**	**3.0 mg/mL**
Wild type *E. coli*	0.9	1.8	2.2	2.7
ΔyliJ-strain	N/I	N/I	N/I	N/I

N/I indicates a field in which no growth inhibition was observed

Chapter 4: Discussion

Glutathione transferases (GSTs) play a major role in protecting cells against a wide variety of exogenous and endogenous small molecule toxicants[12]. GSTs have been purified widely from mammals and their structure, function, and physiological importance have been studied in detail[47, 50]. Nine genes from *Escherichia coli* whose overexpression affords survival in the presence of a normally lethal concentration of the non-natural toxicant bromoacetate have been identified[11]. One of those genes, *yliJ,* encodes a glutathione transferase protein called YliJ. Bacteria which lacked the *ylij* gene become hypersensitive to bromoacetate, which was used to mimic the selective pressures imposed by antibiotics and anthropogenic toxins. Inhibition of YliJ can, therefore, lead to *E. coli* cell death.

In order to explore the potential role of YliJ in detoxication of antibiotics and other toxicants, successful purification and biochemical characterization of YliJ needs to be achieved. The aim of this study was to characterize YliJ biochemically and to develop a simple and safe assay procedure to determine YliJ activity, as compared to the previous research by Desai and Miller[11]. The *E. coli* cells containing the pET20-*ylij* plasmid were grown and protein expression was induced with IPTG. Desai and Miller incorporated a His-tag into the YliJ polypeptide chain; therefore, their purification method involved affinity chromatography with a nickel-nitrilotriacetic acid column[11]. In the current study, *yliJ* was cloned into the expression vector without a tag and a new purification procedure of YliJ was designed. After bacterial cell lysis by sonication, the initial purification of YliJ involved treatment with streptomycin and ammonium sulfate

precipitation. Proteins can be separated from a mixture on the basis of their polarity by increasing the concentration of ammonium sulfate. Partial purification with ammonium sulfate precipitation at 40% and 75% saturation showed little improvement in purity of YliJ. Ammonium sulfate at 40% saturation precipitated appreciable amounts of YliJ along with very few other proteins. Much of the YliJ precipitated at 75% saturation; however, significant amount of YliJ protein still remained in the supernatant even at this high ammonium sulfate concentration (Figure 3-2). This observation is consistent with the prediction that YliJ is considerably hydrophilic[51]. Ammonium sulfate precipitation did not aid significantly in YliJ purification, as both the pellet and supernatant contained appreciable amounts of YliJ protein.

YliJ was further purified with a Fast Flow Q Sepharose ion exchange column. Generally, ion exchange columns are used to separate charged molecules based on the differences in their charge properties. Proteins' charge depends on their isoelectric point, pI, and the pH of the solution. The net charge of a protein is negative or positive if the pH of the buffer is greater or lower than the isoelectric point (pI) of the protein, respectively. The pH of the buffer used for the elution was 6.5. YliJ has a pI of 5.05 and therefore has a net negative charge at pH 6.5. The Q Sepharose matrix is a strong anion exchanger containing positively charged quaternary ammonium groups. As a result, negatively charged YliJ protein will bind to the column, while positively charged proteins will pass through. Bound YliJ was eluted with an increasing gradient of NaCl. Since the ions compete with proteins for binding to the column, bound proteins will elute off the column as the salt concentration increases. The application of the Q Sepharose FF

column resulted in an improvement in YliJ purity (Figure 3-3). Further concentration with the 10, 000 MWCO Amicon Ultra-4 centrifugal unit yielded a more pure YliJ protein as seen on the results of SDS-PAGE analysis (Figure 3-4). The intense band near 23 kD indicates that we have developed a simple purification procedure for YliJ protein that does not contain a His-tag.

The purified YliJ sample was used to determine the kinetic parameters of the enzyme. As neither GSH nor bromoacetate possess spectral characteristics that would allow following the reaction as it progresses, we designed a discontinuous enzymatic assay. In this method we determined the concentration of GSH before and after the reaction with bromoacetate. The rate of the reactions was calculated as a difference between the enzyme-catalyzed and the spontaneous reaction between GSH and bromoacetate. The concentration of GSH was determined using DTNB. DTNB reacts with a free sulfhydryl group of a thiol releasing TNB. Since the amount of thiol reacted is equal to the amount of TNB released, the concentration of thiol is calculated from the absorbance of TNB at 412 nm. Using our assay method, we conducted the steady-state kinetic analysis of YliJ-catalyzed reactions with constant bromoacetate and various GSH concentrations. The enzyme has a Michaelis constant (K_M) of 1.60 mM, a turnover number (k_{cat}) of 175 s^{-1}, and a catalytic efficiency of 1.09×10^5 $M^{-1}s^{-1}$ for the substrate GSH. The kinetic parameters of YliJ with respect to bromoacetate reported by the previous research[11] were: K_M of 5 mM, k_{cat} of 27 s^{-1} and a catalytic efficiency of 5.4×10^3 $M^{-1}s^{-1}$. The lower K_M value recorded in this study shows that YliJ has a higher affinity for GSH than bromoacetate.

The substrate specificity of YliJ was examined by testing the ability of YliJ to catalyze the glutathione-dependent dehalogenation of iodoacetate. Following the same procedure and conditions as in the bromoacetate assay, the kinetic parameters were also determined for YliJ catalyzed conjugation of GSH and iodoacetate. In comparison, the maximum velocity of YliJ-mediated dehalogenation of iodoacetate (2.48 μM/s) was almost the same to the maximum velocity of YliJ-mediated dehalogenation of bromoacetate (2.80 μM/s). This was contrary to the report by Desai and Miler, where the maximum velocity of decomposition of bromoacetate was about 4 times lower than that of iodoacetate[11]. The conjugation of GSH to iodoacetate also increased the affinity of YliJ to GSH (0.175 mM)

The thermostability of the YliJ protein was investigated by incubation of the enzyme at various temperatures for 5 minutes and then testing its enzymatic activity. The highest activity of YliJ was recorded after the incubation of the enzyme at 25 ^{o}C. As shown in Figure 3-7, the activity of the enzyme was not lost even after incubation at 60 °C. This is an indication that the YliJ protein is a relatively stable enzyme. An enzyme's activity is affected by the pH of the assay mixture. To determine the optimal pH of YliJ the purified protein was incubated at 25 ^{o}C with buffers of various pH values and enzyme's activity was found to be the highest at pH 7.0. This confirms previous research[52] that the optimum pH for glutathione transferase from *E. coli* is 7.0. The enzyme was also found to be significantly active from pH 6.0 to 9.0 as shown in Figure 3-8. The plot (Figure 3-8) also shows the typical bell-shaped curve, increasing from the

strong acid region up to a maximum value, and then decreasing in the strong alkaline region[53].

The importance of YliJ in the survival of *E. coli* cells in the presence of halogenated compounds was studied using the *yliJ*-knockout strain of *E. coli* cells. These cells are unable to express YliJ protein since the *yliJ* gene was eliminated from their genome. As shown by the disc-diffusion sensitivity tests (Figure 3-9), the *ylij*-knockout strain was more sensitive to bromoacetate and iodoacetate than the wild type *E. coli*. Based on the diameter of the clearance around the discs, YliJ displays slightly higher specificity towards bromoacetate when compared to other small halogenated compounds. Both the wild type and knockout strains were quite sensitive to iodoacetamide. The inability of the *ylij*-knockout strain *E.coli* to detoxify bromoacetate and iodoacetate shows that YliJ plays a key role in conferring resistance to these halogenated compounds. This also indicates the importance of the carboxylate functional group for YliJ substrate recognition as there was no difference in the sensitivity of both strains to iodoacetamide, the molecule that contains an uncharged amide group instead. This also supports the predictions by previous research[11] that a small molecule containing a carboxylate moiety could be the physiological substrate of YliJ.

It has been reported that glutathione transferase expressed in antibiotic resistant species like *Staphylococcus sp., Streptococcus sp*. and *Micrococcus sp*., plays an important role in protection against the toxic effect of the antimicrobial agents which

leads to antibiotic resistant bacteria[54]. Glutathione transferases have been reported to also detoxify specifically the antibiotic fosfomycin[20]. In this study, the wild type and *ylij*-knockout *E. coli* strains were exposed to three different antibiotics: ampicillin, chloramphenicol, and fosfomycin using the agar disc diffusion method of testing (Figure 3-10).

The sensitivity of both the wild type *E. coli* cells and the knockout strain to fosfomycin was very high compared to ampicillin (Figure 3-10). Surprisingly, with chloramphenicol, the wild type cells were more sensitive than the knockout strain. Usually, chloramphenicol acts by binding to the 50S subunit during translation and ultimately inhibits protein synthesis. The lack of sensitivity of the *ylij*-knockout strain to chloramphenicol may suggest that there are other chloramphenicol inhibitors which only become active in the absence of the *ylij* gene in *E. coli*. This could also mean that the *ylij*-knockout strain was originally chloramphenicol resistant.

Fosfomycin inhibits bacterial cell wall biogenesis by inactivating the enzyme UDP-N-acetylglucosamine-3-enolpyruvyltransferase (MurA). It inhibits MurA by alkylating an active site Cys 115 residue in the *Escherichia coli* enzyme[53]. According to the results (Table 3-3), the knockout strain showed more sensitivity to fosfomycin. The increase in sensitivity to fosfomycin by the cells lacking *ylij* suggest that the protein produced from the *ylij* gene may play a role in protecting MurA enzyme from being inactivated by fosfomycin and other bacterial cell wall biogenesis inhibitors.

The wild type *E. coli* cells were more resistant to ampicillin while the knockout strain showed some sensitivity to this antibiotic (Table 3-3). Ampicillin causes cell lysis by inhibiting the third and final stage of bacterial cell wall synthesis in binary fission[53]. The increased resistance in the wild type suggests that YliJ may function in protecting bacterial cell wall lysis.

Future Work

Future work will include exploring different purification techniques in purifying YliJ. The kinetic parameters of the enzyme for varying bromoacetate concentration and constant GSH will be determined. YliJ catalyzed reactions will also be analyzed qualitatively with respect to halogenated compounds using HPLC-based assay method. In addition, YliJ will be further characterized using other halogenated compounds or non-halogenated compounds with similar properties. The catalytically important residues predicted for YliJ will also be verified using site-directed mutagenesis.

Chapter 5: Conclusion

A safe simple activity assay has been developed for YliJ and characterization of the enzyme was also accomplished. Partial purification was achieved using ammonium sulfate precipitation, and a Q Sepharose FF anion exchange column. The kinetic parameters of YliJ were determined using the purified enzyme. YliJ has a K_M of 1.60 mM, a k_{cat} of 175.0 s^{-1} and a catalytic efficiency of 1.09×10^5 $M^{-1}s^{-1}$ for GSH when conjugated to bromoacetate. In comparison, YliJ has a K_M of 0.1753 mM, a k_{cat} of 155.3 S^{-1} and a catalytic efficiency of 8.86×10^4 $M^{-1}s^{-1}$ for GSH when conjugated to iodoacetate. An improved purification should be developed in order to accurately determine the kinetic parameters of YliJ. YliJ was found to be significantly stable even at 60 ^oC and from pH 6.0 to 9.0. The optimum pH for YliJ activity was confirmed to be pH 7.0.

E. coli cells expressing YliJ protein and the knockout strain BW25113Δ*yliJ* lacking YliJ were tested for sensitivity to halogenated compounds and antibiotics. It was found that, the *E.coli* cells expressing YliJ protein were more resistant to bromoacetate and iodoacetate than the *yliJ*-knockout strain. The ability of the wild type *E.coli* to detoxify bromoacetate and iodoacetate shows that YliJ may play a key role in conferring resistance to these halogenated compounds. The results strongly support the suggestion that a small molecule containing a carboxylate moiety could be the physiological substrate of YliJ. For antibiotic sensitivity, it was found that the *ylij*-knockout strain showed higher sensitivity to fosfomycin than the wild type. There was an increase in sensitivity to ampicillin in the *ylij*-knockout strain as compared to the wild type *E. coli* cells indicating that YliJ may function in protecting bacterial cell wall lysis by

exogenous substances. With chloramphenicol, the wild type cells were more sensitive than the knockout strain. Further studies are required to understand these observations.

Chapter 6: Reference

1. G. V. Smirnova, O. N. Oktyabrsky**.** Glutathione in Bacteria, *Biochemistry (Moscow).* **2005**, *70*, 1199–1211.

2. H. Sies. Glutathione and its role in cellular functions. *Free Radical Biol Med*. **1999**, *27*, 916-921.

3. J. D. Reed. Glutathione: Toxicological Implications. *Annu Rev Pharmacol Toxicol*. **1990**, *30*, 603-631.

4. R. C. Fahey, W. C. Brown, W. B. Adams, and M. B. Worsham. Occurrence of glutathione in bacteria. *J Bacteriol*. **1978**, *133*, 1126-1129.

5. G. L. Newton, K. Arnold, M. S. Price, C. Sherrill, S. B. Delcardayre, Y. Aharonowitz, G. Cohen, J. Davies, R. C. Fahey, and C. Davis. Distribution of thiols in microorganisms: mycothiol is a major thiol in most actinomycetes. *J Bacteriol*. **1996**, *178 (7)*, 1990-1995

6. Sherrill, C., and Fahey, R. C. Import and Metabolism of Glutathione by *Streptococcus* mutans. *J Bacteriol*. **1998**, *180 (6)*, 1454-1459.

7. B. Vergauwen, F. Pauwels, M. Vaneechoutte, and J. J. Van Beeumen. Exogenous Glutathione Completes the Defense against Oxidative Stress in *Haemophilus influenza*. *J Bacteriol*. **2003**, *185 (5)*, 1572-1581.

8. A. R. Sundquist, and R. C. Fahey. Evolution of Antioxidant Mechanisms: Thiol-Dependent Peroxidases and Thioltransferase among Prokaryotes. *J Mol Evol*. **1989**, *29*, 429-435.

9. C. Ufer and C. C. Wang. The roles of glutathione peroxidases during embryo development. *Front Mol Neurosci*. **2011**, *4*(12), 1-12.

10. G. V. Smirnova, T. A. Krasnykh, O. N. Oktyabrsky. Role of Glutathione in the Response of *Escherichia coli* to Osmotic Stress. *Biochemistry (Moscow)*. **2001**, *66*, 973-978.

11. K. K. Desai, B. G. Miller. Recruitment of genes and enzymes conferring resistance to the non-natural toxin bromoacetate. *PNAS.* **2010**, *107*, 17968–17973.

12. D. M. Townsend, K. D. Tew. The role of glutathione-S-transferase in anti-cancer drug resistance. *Oncogene.* **2003**, *22*, 7369–7375.

13. J. D. Hayes, J. U. Flanagan and I. R. Jowsey. Glutathione transferases. *Annu Rev Pharmacol Toxicol*. **2005**, *45*, 51–88.

14. R. N. Armstrong. Mechanistic diversity in a metalloenzyme superfamily. *Biochemistry. **2000,** 39*, 13625–13632.

15. A. A. Enayati, H. Ranson, and J. Hemingway. Insect glutathione transferases and insecticide resistance*. Insect Biochem Molec Biol.* **2005***, 14,* 3-8.

16. D. Sheehan, G. Meade, V. M. Foley and C. A. Dowd. Structure, function and evolution of glutathione transferases: implications for classification of non-mammalian members of an ancient enzyme superfamily*. Biochem J.* **2001***, 360,* 1–16.

17. A. Robinson, G. A. Huttley, H. S. Booth and P. G. Board. Modelling and bioinformatics studies of the human kappa-class glutathione transferase predict a novel third glutathione transferase family with similarity to prokaryotic 2-hydroxychromene-2-carboxylate isomerases. *Biochem J*. **2004**, *379*, 541–552.

18. P. J. Jakobsson, R. Morgenstern, J. Mancini, A. Ford-Hutchinson and B. Persson. Common structural features of MAPEG – a widespread superfamily of membrane-associated proteins with highly divergent functions in eicosanoid and glutathione metabolism. *Protein Sci*. **1999**, *8,* 689–692.

19. R. C. Strange, M. A. Spiteri, S. Ramachandran, A. A. Fryer. Glutathione-S-transferase family of enzymes. *Mutat Res.* **2001**, *482*, 21–26.

20. J. D. Hayes and D. J. Pulford. The glutathione S-transferase supergene family: regulation of GST and the contribution of the isoenzymes to cancer chemoprotection and drug resistance. *Crit Rev Biochem Mol Biol.* **1995**, *30*, 445-600.

21. A. G. Clark, J. N. Smith, and T. W. Speir. Cross specificity in some vertebrate and insect glutathione-S-transferases with methyl parathion (dimethyl-p-nitrophenyl phosphorothionate), 1-chloro-2, 4-dinitrobenzene and S-crotonyl-N-acetylcysteamine substrates. *Biochem J.* **1973**, *135*, 385-392.

22. J. Rossjohn, G. Polekhina, S. C. Feil, N. Allocati, M. Masulli, C. Di Ilio and M. W. Parker. A mixed disulfide bond in bacterial glutathione transferase: functional and evolutionary implications. *Structure.* **1998***, 15*, 721–734.

23. S. Vuilleumier. Bacterial Glutathione S-Transferases: What Are They Good for? *J Bacteriol.* **1997**, *179* (5), 1431–1441

24. D. Sheehan, G. Meade, V. M. Foley, C. A. Dowd. Structure, function and evolution of glutathione transferases: implications for classification of non-mammalian members of an ancient enzyme superfamily. *Biochem J*. **2001**, *360*, 1-16.

25. S. C. Feil, J. Tang, G. Hansen, M. A. Gorman, E. Wiktelius, G. Stenberg, M. W. Parker. Crystallization and preliminary X-ray analysis of glutathione transferases from cyanobacteria. *Acta Cryst*. **2009**, F*65*, 475-477.

26. N. V. Stourman, M. C. Wadington, M. R. Schaab, H. J. Atkinson, P. C. Babbitt, R. N. Armstrong. Functional Genomics in *Escherichia coli*: Experimental Approaches for the Assignment of Enzyme Function. Proceedings of "3rd International ESCEC Symposium on Experimental Standard Conditions on Enzyme Characterizations" Sept. 23rd - 26th, 2007, Ruedesheim, Germany, p.1-12.

27. T. Kanai, K. Takahashi, and H. Inoue. Three distinct-type glutathione S-transferases from *Escherichia coli* important for defense against oxidative stress. *J Biochem*. **2006**, *140*, 703–711.

28. N. V. Stourman, M. C. Branch, M. R. Schaab, J. M. Harp, J. E. Ladner, and R. N. Armstrong. Structure and Function of YghU, a Nu-Class Glutathione Transferase Related to YfcG from *Escherichia coli*. *Biochemistry*. **2011**, *50*, 1274–1281.

29. S. Vuilleumier, N. Ivoš, M. Dean, T. Leisinger. Sequence variation in dichloromethane dehalogenases/glutathione S-transferases. *Microbiology*. **2001a**, *147*:611–619.

30. S. Vuilleumier, and M. Pagni. The elusive roles of bacterial glutathione S-transferases: New lessons from genomes. *Appl Microbiol Biotechnol*. **2002**, *58*, 138–146.

31. J. D. Hayes and L. I. McLellan. Glutathione and glutathione-dependent enzymes represent a co-ordinately regulated defence against oxidative stress. *Free Radical Res.* **1999**, *31*,273-300.

32. B. Mannervik. Glutathione and the evolution of enzymes for detoxication of products of oxygen metabolism. *Chem Scripta*. **1986**, *26B*, 281–284.

33. B. Ketterer, J. M. Harris, G. Talaska, D. J. Meyer, S. E. Pemble, J. B. Taylor, N. P. Lang, and F. F. Kadlubar. The human glutathione S-transferase supergene family, its polymorphism, and its effects on susceptibility to lung cancer. *Environ. Health Perspect*. **1992**; *98*: 87–94.

34. G. Litwack, B. Ketterer, and I. M. Arias. Ligandin: a hepatic protein which binds steroids, bilirubin, carcinogens, and a number of exogenous anions. *Nature (London).* **1971**, *234*, 466-467.

35. K. D. Tew, C. B. Pickett, T. J. Mantle, B. Mannervik and J. D. Hayes. Structure and Function of Glutathione Transferases, *CRC Press, Boca Raton, FL*, **1993**, pp. 199-209.

36. K. A. Marrs. The functions and regulation of glutathione S-transferases in plants. *Annu Rev Plant Physiol Plant Mol Biol*. **1996**, *47*:127–158.

37. F. Toribio, E. Martinez-Lara, P. Pascual, J. Lopez-Barea. Methods for purification of glutathione peroxidase and related enzymes. *J Chromatogr B Biomed Appl*. **1996**; *684*(1-2):77-97.

38. Y. Urade, K. Watanabe and O. Hayaishi. Prostaglandin D, E, and F synthase. *J. Lipid Mediat Cell Signal* **1995**, *12*, 257-273.

39. J. M. Fernandez-Canon and M. A. Penalva. Characterization of a fungal maleylacetoacetate isomerase gene and identification of its human homologue. *J Biol Chem.* **1998**, *273*, 329-337.

40. A. M. Benson, P. Talalay, J. H. Keen and W. B. Jakoby. Relationship between the soluble glutathione-dependent 5 -3-ketosteroidisomerase and the glutathione S-transferases of the liver. *Biochemistry*: *Proceedings of the National Academy of Sciences, USA*, **1977**, *74 (1)*, 158-162.

41. H. Chen and M. R. Juchau. Glutathione S-transferases act as isomerases in isomerization of 13-cis-retinoic acid to all-trans-retinoic acid in vitro. *Biochem J*. **1997**, *327*, 721-726.

42. P. J. Sherratt and J. D. Hayes. Glutathione S-transferases, in Enzyme Systems that Metabolize Drugs and Other Xenobiotics. **2001**, John Wiley & Sons, Ltd, Chichester, UK, pp. 1-34.

43. F. P. E. Guengerich, E. M. J. Gillam, and T. Shimada. New applications of bacterial systems to problems in toxicology. *Crit Rev Toxicol*. **1996**, *26*: 551–583.

44. L. A. Kelly *et al.* The Phyre2 web portal for protein modeling, prediction and analysis. *Nature Protocols,* **2015***, 10,* 845-858.

45. D. M. Maron, and B. N. Ames. Revised methods for the *Salmonella* mutagenicity test. *Mutat Res*. **1983**, *113*: 173–215.

46. M. Arifuzzaman, M. Maeda, A. Itoh, K. Nishikata, C. Takita, R. Saito, T. Ara, K. Nakahigashi, H. C. Huang, A. Hirai, K. Tsuzuki, S. Nakamura, M. Altaf-Ul-Amin, T. Oshima, T. Baba, N. Yamamoto, T. Kawamura, T. Ioka-Nakamichi, M. Kitagawa, M. Tomita, S. Kanaya, C. Wada, H. Mori. Large-scale identification of protein-protein interaction of *Escherichia coli* K-12. *Genome Res*. **2006**. *16*, 686-691.

47. R. N. Armstrong. Structure, Catalytic Mechanism and Evolution of the Glutathione Transferases. *Chem Res Toxicol*. **1997**, 10, 2 – 18.

48. D. L. Eaton, T. K. Bammler. Concise review of the glutathione S-transferases and their significance to toxicology. *Toxicol Sci*. **1999**, *49*: 156–64.

49. M. Nishida, S. Harada, S. Noguchi, Y. Satow, H. Inoue, K. Takahashi. Three-dimensional structure of *Escherichia coli* glutathione S-transferase complexed with glutathione sulfonate: catalytic roles of Cys10 and His106. *J Mol Biol*. **1998**, 281: 135–147.

50. G. J. Beckett and J. D. Hayes. Glutathione S-transferases: biomedical applications. **1993**, *Adv. Chim. Chem*. **30**, 281-380.

51. http://www.uniprot.org/uniprot/P0ACA7.

52. W. A. Petri, B. A. Chabner, B. C. Knollmann. Goodman and Gilman's the Pharmacological Basis of Therapeutics, **2011**, 12th ed., Chapter 53. McGraw-Hill, New York.

53. E. D. Brown, E. I. Vivas, C. T. Walsh, and R. Kolter. "MurA (MurZ), the enzyme that catalyzes the first committed step in peptidoglycan biosynthesis, is essential in *Escherichia coli*". *J Bacteriol*. **1995**, *177* (14), 4194–4197.

54. K. Thamaraiselvi. Expression of Glutathione S-transferase in antibiotic resistance bacterial species (*Staphylococcus sp., Streptococcus sp. and Micrococcus sp*.) isolated from the poultry litter. “World Congress on Biotechnology”, March 21st-23rd, 2011, NICC Nyderabad, India.